Geology of southern Black Mesa, Espanola Basin, New Mexico: New stratigraphic age control and interpretation of the southern Embudo fault system of the Rio Grande rift

Daniel J Koning, William McIntosh, and Nelia Dunbar, 2011, pp. 191-214

Supplemental data available: http://nmgs.nmt.edu/repository/index.cfm?rid=2011001

in:

Geology of the Tusas Mountains and Ojo Caliente, Author Koning, Daniel J.; Karlstrom, Karl E.; Kelley, Shari A.; Lueth, Virgil W.; Aby, Scott B., New Mexico Geological Society 62nd Annual Fall Field Conference Guidebook, 418 p.

This page is intentionally left blank to maintain order of facing pages.

New Mexico Geological Society Guidebook, 62nd Field Conference, Geology of the Tusas Mountains - Ojo Caliente, 2011, p. 191-214.

GEOLOGY OF SOUTHERN BLACK MESA, ESPAÑOLA BASIN, NEW MEXICO: NEW STRATIGRAPHIC AGE CONTROL AND INTERPRETATIONS OF THE SOUTHERN EMBUDO FAULT SYSTEM OF THE RIO GRANDE RIFT

DANIEL J. KONING[1], WILLIAM MCINTOSH[1] AND NELIA DUNBAR[1]
[1]New Mexico Bureau of Geology and Mineral Resources, New Mexico Institute of Mining and Technology, 801 Leroy Place, Socorro, NM 87801

Abstract—Studies involving geologic mapping, tephrochronology, and $^{40}Ar/^{39}Ar$ dating on southern Black Mesa have increased our understanding of late Miocene through Pliocene deposition and tectonism at the center of the Española Basin. A prominent landmark extending 21 km in a northeast direction, Black Mesa is capped by 3-20 m of 3.3-3.8 Ma Servilleta Basalt flows and forms a prominent landmark north of Española. These basalts overlie 1-20 m of Pliocene strata, including ancestral Rio Grande sediment. The Pliocene strata unconformably overlie upper Miocene strata of the Chamita Formation (Santa Fe Group). Strata pre-dating the Chamita Formation include the Ojo Caliente Sandstone Member of the Tesuque Formation (Santa Fe Group), which was deposited in an extensive dune field. The margin of this dune field retreated north-northwestward between 11.0-11.5 and 9-10 Ma, concomitant with fluvial deposition by an ancestral Rio Grande (Vallito Member of Chamita Formation) and an unnamed river flowing southwest from the Peñasco embayment (Cejita Member of Chamita Formation). After 8 Ma, the distal toe of eastern piedmont-slope sediment (Cuarteles Member of the Chamita Formation) advanced westward to under the present-day mesa. Several faults and folds in the vicinity of Black Mesa include the northeast-striking Santa Clara and La Mesita faults of the Embudo fault system, the southern Ojo Caliente fault, and the west-plunging Chamita syncline. Pliocene strata thicken eastward across the Santa Clara fault, consistent with vertical displacement during Pliocene time. High slip rates on the southern Embudo fault system and the Chamita syncline occurred between 7-8 Ma (age of lower and upper Chamita tuffaceous zones) and 3.3-3.8 Ma (age of the Servilleta Basalt), based on a pronounced contrast in dips across an angular unconformity between these two stratums. An angular unconformity at the base of Pliocene strata correlates to an unconformity at the base of the 2-5 Ma Puyé Formation to the south, and supports tectonic tilting and deformation, but relatively low sediment preservation, between 3.8 and 6 Ma. Activity on the southern Embudo fault system and Chamita syncline decreased after 3.3-3.8 Ma. Slower tectonic subsidence of the basin and increased discharges along the adjacent Rio Grande and Rio Chama during the Pleistocene induced deep erosion of weakly resistant Santa Fe Group strata and resulted in topographic inversion of the basalt-capped Black Mesa.

INTRODUCTION

Black Mesa forms a prominent landmark north of Española and is located in the Española Basin of the Rio Grande rift (Fig. 1). Extending 21 km in a northeast direction, it is capped by a 3-20 m-thick package of Servilleta Basalt flows. The mesa lies between the Rio Grande and Rio Ojo Caliente, and the Rio Chama lies only 1 km from the south end of the basalt (Figs. 1-2). Black Mesa overlies one of the structurally deeper parts of the Española Basin, the Velarde graben of Manley (1979a), based on gravity and seismic reflection data (Ferguson et al., 1995; Koning et al., 2004a). The Velarde fault bounds the east side of this graben and the La Mesita fault strikes through the middle of the graben (Koning et al., 2004a). Both of these faults belong to the Embudo fault system, whose faults collectively act as a major transfer structure in accommodating extension between the Española Basin and the adjoining San Luis Basin to the northeast (Muehlberger, 1978 and 1979; Faulds and Varga, 1998). To the west of Black Mesa lies the Abiquiu embayment, which is a faulted structural platform overlain by 1 km of basin-fill (Baldridge et al., 1994; Koning et al., 2004a). This paper focuses on the geology of the southern 9 km of Black Mesa. We describe the geologic structure and then the Miocene strata (i.e., Tesuque Formation and overlying Chamita Formation), Pliocene sediment, and the Servilleta Basalt. We argue for a diachronous, 11-9 Ma minimum age for the Ojo Caliente Sandstone Member of the Tesuque Formation using tephrochronology, and present new $^{40}Ar/^{39}Ar$ ages determinations for the Servilleta Basalt. The paper concludes with paleogeographic and tectonic interpretations that highlight lateral shifts of three fluvial systems and an eolian dune field, as well as high slip rates along the southern Embudo fault system, during the late Miocene and early Pliocene.

STRUCTURE

Santa Clara fault

The main geologic structure at the southern tip of Black Mesa is the north end of the Santa Clara fault (Figs. 1 and 2). Considered part of the Embudo fault zone (Aldrich, 1986; Aldrich and Dethier, 1990; Koning et al., 2004a), the Santa Clara fault extends 20 km between here and its southern end at Santa Clara Canyon. South of the Rio Chama, the Santa Clara fault is characterized by a wide zone (hundreds of meters) of steeply southeast-dipping to overturned beds of the Chamita Formation. At the southern tip of Black Mesa, two strands of the Santa Clara fault are interpreted within 0.8 km east of the eastern edge of the Servilleta Basalt. Based on a WNW cross-section, the two strands have stratigraphically offset an inferred 10.5-11.0 Ma tephra bed(s) ~350 m down-to-the-southeast (Fig. 3; Koning et al., in review). Kinematic indicators observed south of the Rio Chama indicate both right- and left-lateral slip (Aldrich, 1986; Aldrich and Dethier, 1990; Gonzales, 1993; Minor et al., in review, fig. 4d; Koning et al., in review). We infer the dominant sense of

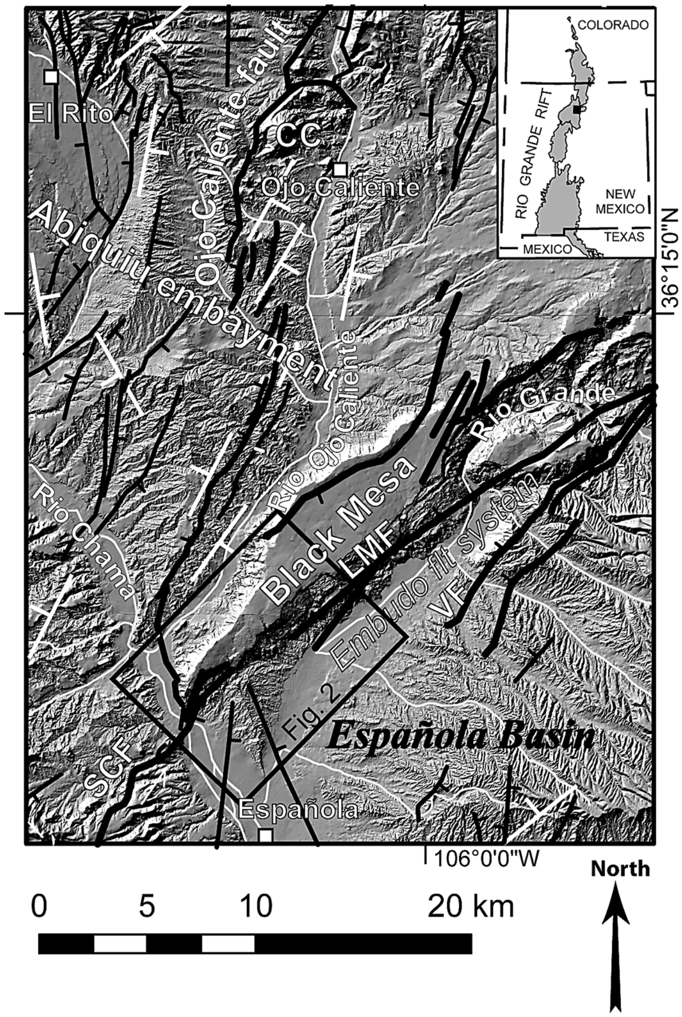

FIGURE 1. Shaded relief map showing the location of Black Mesa in the northern Española Basin. Towns and cities are depicted by white squares outlined in black. Faults are shown as thick black lines, with tic marks on the down-thrown side of faults. Representative strikes and dips of strata are drawn in white. Major streams and rivers are illustrated by thin, white lines. Black rectangle shows the study area and the location of Fig. 2. Small map in top right corner of figure shows the position of the study area within the Rio Grande rift. CC = Cerro Colorado; LMF = La Mesita fault; VF = Velarde fault; SCF = Santa Clara fault.

slip to be left-lateral, given the east-west extension direction of late rifting and the presence of the La Mesita fault 1-2 km to the east of its north end (the La Mesita fault has a strong left-lateral component of slip, as noted below). Another strand of the Santa Clara fault likely strikes along the northwestern edge of the mesa (Figure 2), based on a steep gravity gradient there (Ferguson et al., 1995; Koning et al., 2004a). However, this fault strand does not offset poorly-exposed strata in this area and appears to have been inactive for the past 10 Ma.

Although not exposed, the Santa Clara fault is evidenced by steeply dipping strata and the juxtaposition of various lithologic units (Figs. 2 and 3). Miocene strata dip steeply on the immediate fault footwall near the Rio Chama (13-54° E), but dip less steeply (4-9° SE) 2 km northwest of the mapped end of the Santa Clara fault (Figs. 2 and 3). Normal displacement of the Servilleta Basalt is easily recognized from a distance (Fig. 4). Within 3 km from north to south, stratigraphic displacement of the basalt increases from 0 to 115 m on the western fault strand and from 0 to 65-70 m on the eastern strand. At the beginning of senior author's field work here (early 2003), it was thought that the down-dropped basalt was due to mass-wasting, which is very prominent on the east slope of Black Mesa to the north as Toreva block landsliding. We prefer a tectonic process for the displaced basalt because: 1) the Santa Clara fault clearly extends to here, based on offset upper Miocene strata immediately south of the displaced basalt and north of the Rio Chama, 2) the displaced basalt is not extensively fractured or back-tilted, as is typical in the Toreva block landslides to the north, 3) the basalt in the hanging wall extends 3-4 km along the fault in a relatively continuous fashion, and 4) mapping reveals a continuous stratigraphic succession below the basalts; thus, any landslide basal shear plane would have to extend well below the present elevation of the Rio Chama, which represents the lowest base level west of the Rio Grande since the beginning of the Pleistocene (note that 10-20 m of latest Pleistocene-Holocene alluvium likely underlies the Rio Chama). The Santa Clara fault has been active in the late Miocene through Quaternary, but throw rates have decreased since 3-4 Ma (Koning et al., in review).

Ojo Caliente and La Mesita faults

The Ojo Caliente fault is a major down-to-the-northwest fault zone that extends 35 km northeast towards Ojo Caliente (Fig. 1). Southwest of the town, it steps to the northwest and is mapped north along the western flank of the basement-cored Cerro Colorado (Fig. 1). In the study area, the south end of the fault bends to the southeast and seems to converge with the Santa Clara fault (Figs. 1 and 2). This fault was called the Chili fault by Koning et al. (2004), but further mapping strongly suggests that the fault is actually a southern extension of the Ojo Caliente fault, so the name Chili fault is hereby abandoned. In contrast to the Santa Clara fault, the Ojo Caliente fault is a down-to-the-west normal fault with a slight component of left-lateral motion (May, 1980; Koning et al., 2004a).

Four to five kilometers east-southeast of the north end of the Santa Clara fault lies the south end of the northeast-striking La Mesita fault, also part of the Embudo fault system (Figs. 1 and 2; Koning et al., 2004a). Although the sense of dominant lateral slip on the Santa Clara fault is ambiguous south of the Rio Chama (based on outcrop-scale kinematic indicators), the northeast-striking Embudo fault system is clearly left-oblique (Steinpress, 1980 and 1981; Leininger, 1982; Hillman, 1986; Hall, 1988; Bradford, 1992; K. Kelson et al., unpubl, report for the U.S. Geological Survey, 1997; Kelson et al., 2004; Koning et al., 2004a).

Folds

East of the north end of the Santa Clara fault, the Santa Fe Group is deformed by the southwest-plunging Chamita syncline (Fig. 2; Koning and Manley, 2003; Koning et al., 2004a). Dips on the south limb of the syncline are 2 to 54° NNE and dips on the

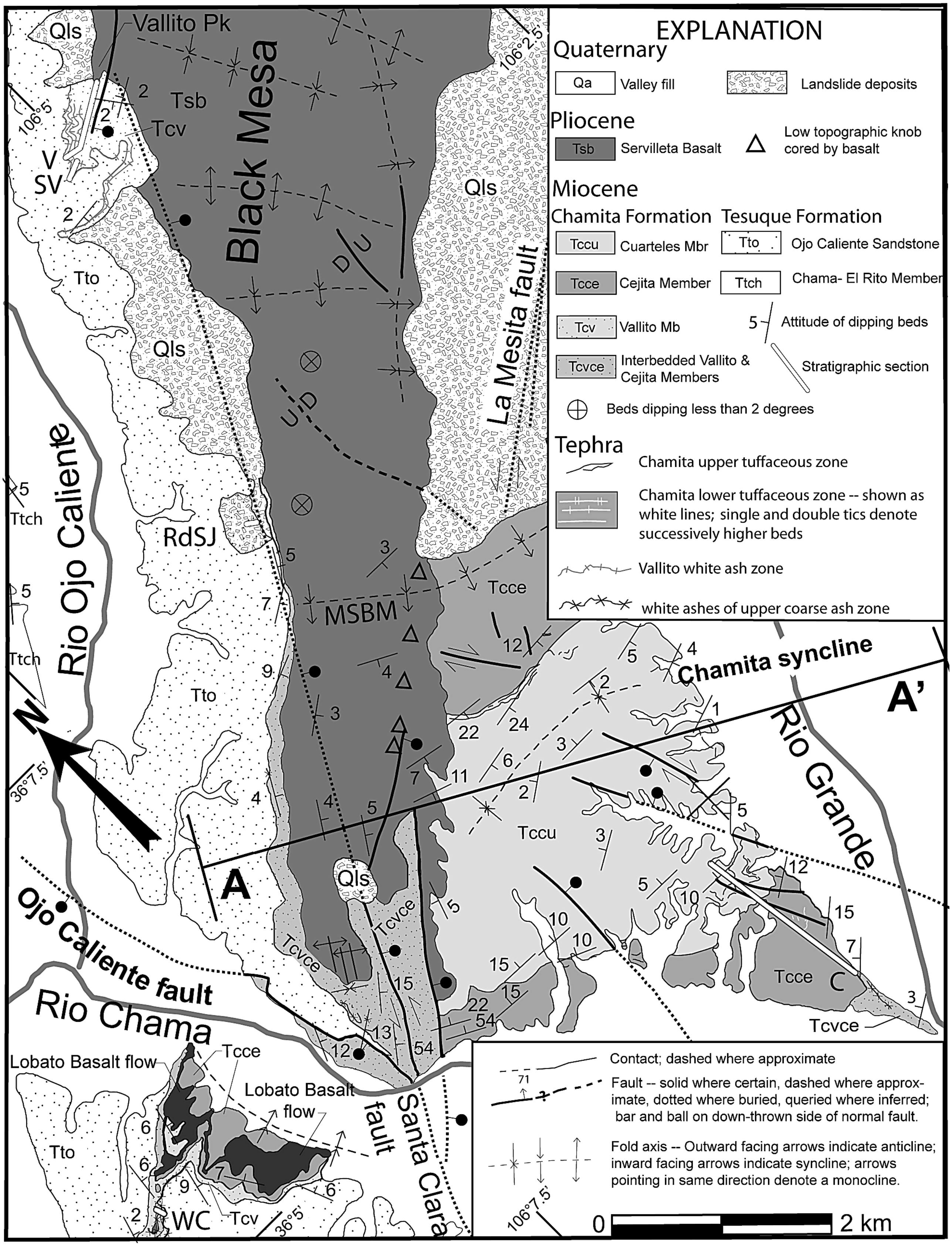

FIGURE 2. Geologic map of the study area (constructed from Koning and Manley, 2003, Koning, 2004, and Koning et al., 2005a). Note that true north is rotated 44 degrees left of vertical. Cross-section A-A’ is shown in Fig. 3. MSBM = monocline of southern Black Mesa. Abbreviations of stratigraphic sections are as follows: WC = West Chili; RdSJ = Rancho de San Juan; SV = South Vallito; V = Vallito; C = Chamita.

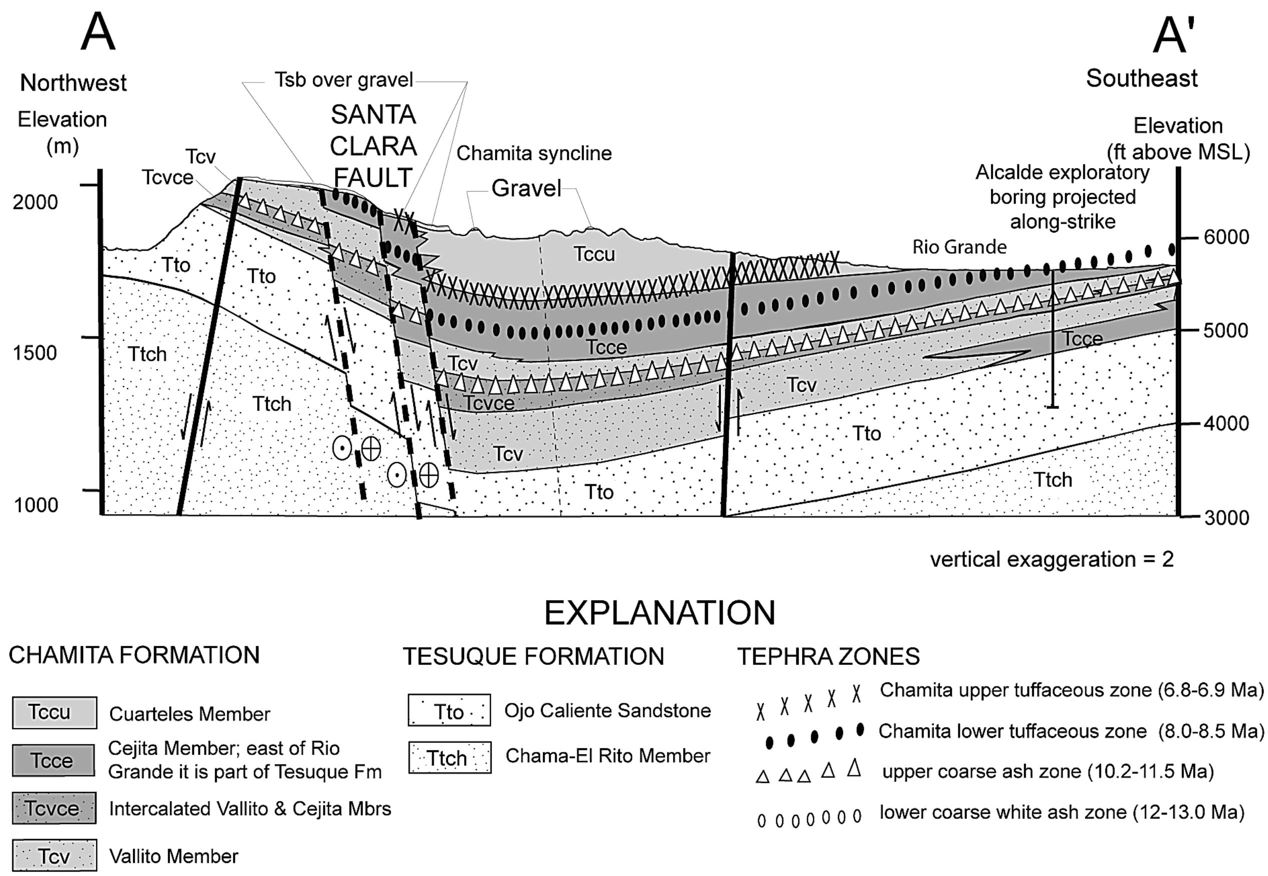

FIGURE 3. Cross-section A-A', which trends northeast through southern Black Mesa. Its location is shown in Fig. 2.

north limb of the syncline are 4 to 27° S. Dips on both limbs of the syncline are steepest immediately adjacent to the east strand of the Santa Clara fault, with dips on the north limb increasing progressively westward more than on the south limb (Fig. 2).

The monocline of southern Black Mesa (MSBM on Fig. 2) is a south-down flexure that trends 290°, dips south, and aligns with the north limb of the Chamita syncline. This fold may represent late-stage deformation related to the Chamita syncline. The monocline has displaced the upper surface of the Servilleta Basalt 50-60 m down-to-the-south; this surface dips 3-4° S on the monocline limb and corresponds with the modern topographic surface (Koning and Manley, 2003). The upper surface of the Servilleta Basalt south of the monocline dips 3-5° E. East of Vallito Peak, the topographic expression of the top of the Servilleta Basalt implies two northwest-trending anticlines on either side of a northwest-trending syncline (Fig. 2). These inferred folds do not appear to extend to the west edge of the mesa, where there is no topographic expression of these folds and the base of the Servilleta basalt is not deformed.

The Servilleta Basalt is folded at the southernmost tip of Black Mesa into two northeast-striking synclines separated by an anticline (Figs. 2 and 5). The amplitude of these folds ranges from 5-10 m. The hillslope below the basalt is covered by talus and we could not determine the magnitude of folding in the underlying Chamita Formation.

GEOCHRONOLOGY

Tephrochronology

A sample from an ash in the Ojo Caliente Sandstone of the Tesuque Formation (sample ML-482L-101103-djk) was analyzed by electron microprobe at the New Mexico Institute of Mining and Technology. Samples were mounted in epoxy, polished flat, and then examined using backscattered electron imaging (BSE). Selected glass particles were quantitatively analyzed. The method that we have chosen to compare this tephra with a dataset of other analyzed tephra, which is only applicable to compositionally homogenous tephra layers, involves calculation of the Euclidean distance function, D (in standard deviation units), between chemical analyses (Perkins et al., 1995). The distance function takes into account the analytical error on the analyses, and therefore more heavily weights elements with higher analytical precision. In the case of the analyses presented in this study, the elements that are used in the statistical difference calculations are Fe, Ca, Ti, Mg, Mn and K. The precision on determinations of Si, Al, P, Na and F tends to be lower, either due to analytical constraints, low abundances, or, as in the case of Na, volatility under the beam (particularly at small beam sizes), so these elements are not included. If two analyses were perfectly identical,

FIGURE 4. Photograph of southern Black Mesa, looking west. The east strand of the Santa Clara fault corresponds to the thick, white line. The thin, white line locally drawn at the base of the Servilleta Basalt illustrates the southward increase of vertical displacement along the fault. The white arrow marks the monocline of southern Black Mesa.

the D value would be 0. However, because of normal statistical error of techniques used for shard analysis, the mean composition of two, coarse-grained, chemically identical tephra samples, such as those analyzed in this study, will typically have a D value of around 4 (Perkins et al., 1995). Any value below 10 suggests a high degree of similarity between samples. The details of the electron microprobe analysis of sample ML-482L-101103-djk are summarized in Table 1 and indicate a strong correlation to the Cougar Point Tuff Unit Xl, a Trapper Creek Ash (M. Perkins, 2001, personal commun.; composition data of Perkins et al., 1995).

$^{40}Ar/^{39}Ar$ Geochronology

Five samples from the Black Mesa area were dated by $^{40}Ar/^{39}Ar$ methods at the New Mexico Geochronology Research Laboratory (Table 2). Dated samples include one biotite-bearing tephra from the lower Chamita Formation and four samples of basaltic lava from the Servilleta Basalt on Black Mesa. One biotite separate and four groundmass concentrates were prepared from these samples using crushing, grinding, sieving, ultrasonic washing, Franz magnetic separation, and hand-picking techniques. Samples were then irradiated along with Fish Canyon Tuff sanidine (28.02 Ma, Renne et al, 1998). $^{40}Ar/^{39}Ar$ analyses were performed using a

FIGURE 5. Photograph of the southern tip of Black Mesa, view is to the north. Arrows point to two synclines on either side of an anticline.

Mass Analyzer Products 215-50 mass spectrometer on line with an automated all-metal extraction system. Analytical parameters and results are summarized in Appendices 1-2 and additional analytical methods are given in Koning et al. (in review, appendix C). Single grains of biotite were step-heated in two to three steps using a 50 watt CO2 laser. Bulk samples (88 to 115 mg) of groundmass concentrate were step heated in ten steps in a molybdenum double-vacuum resistance furnace.

The five analyzed samples yielded results of varying quality. Age spectra (Fig. 6) from two basalt samples (V-63-061103-djk and 110604c-djk) are generally flat, yielding relatively precise plateau ages (3.53 ± 0.25 Ma and 3.34 ± 0.32 Ma respectively). Intercept ages from isochron analyses (Appendix 1) are not significantly different from the plateau ages and $^{40}Ar/^{36}Ar$ intercepts are within error of atmospheric values, indicating that the results are probably not significantly influenced by excess ^{40}Ar. The plateau ages from these two samples are interpreted as accurate eruption ages. The remaining two basalt groundmass concentrates (V-31-041103-djk and 110604b-djk) yielded age spectra (Fig. 6) that are disturbed and have generally low radiogenic yields. Accurate eruption ages were not determined for these samples. For the tephra, high temperature step analyses from the individual biotite grains yielded a unimodal distribution of ages with a weighted mean age of 11.08 ± 0.44 Ma (Fig. 7; Appendix 2), which is interpreted as a moderately accurate eruption age for the sampled ash layer, given that some volcanic biotites are notorious for yielding apparent ages as much 500 ka older than eruption ages determined by other means (Bacmann et al., 2010; Hora et al., 2010). Subsequent sections discuss the significance of the age results presented above.

STRATIGRAPHY

Miocene strata

Older strata on footwall of Santa Clara fault

Strata of the Chamita and Tesuque Formations (Galusha and Blick, 1971) unconformably underlie Pliocene sediment on the

TABLE 1. Average chemical composition (in wt.%) of shards of sample ML-482L, and representative compositions of suggested correlative tephra

Sample Number	n	P_2O_5	SiO_2	SO_2	TiO_2	Al_2O_3	MgO	CaO	MnO	FeO	Na_2O	K_2O	F	Cl	estimated grain size (microns)¥	Interpreted correlation
ML-482L-101103-djk*	20	**0.01**	**76.45**	**0.01**	**0.22**	**12.31**	**0.04**	**0.66**	**0.03**	**1.88**	**2.42**	**5.74**	**0.15**	**0.05**	100	Cougar Point Tuff of Unit Xl
standard deviation		0.02	0.42	0.01	0.03	0.16	0.01	0.06	0.02	0.09	0.26	0.30	0.07	0.01		(D=3.97)
Known tephra compositions																
Cougar Point Tuff Unit XI **			76.57		0.21	11.96	0.05	0.61	0.03	1.81	2.31	6.19	0.22	0.04		

Notes:

Analyses are normalized to 100% oxide total.

Location of sample (UTM coord, NAD 27, zone 13): 401220 m E, 3998420 m N

* Analysed at New Mexico Tech with the following analytical conditions: accelerating voltage of 15 kV and probe current of 10 nA. Peak count times of 20 seconds were used for all elements with the exception of Na (40 sec), F (100 sec), cl (40m sec) and S (40 sec).

Background counts were obtained using one half the times used for peak counts. Analyses are normalized to 100 wt.%. N equals number of analyses. Analytical precision, based on replicate analyses of standard reference materials of similar composition to the unknows, are as follows (all in wt.%): P2O5±0.02, SiO2±0.47, SO2±0.01, TiO2±0.03, Al2O3±0.12, MgO±0.07, CaO±0.02, MnO±0.06, FeO±0.06, Na2O±0.55, K2O±0.27, cl±0.07.

** Sample TC89-27c (Perkins et al., 1995)

¥Grain size estimates are qualitative. The number given is the estimated size of The largest population of shards

south part of Black Mesa. The older part of the stratigraphic section is exposed on the upthrown, western side of the Santa Clara fault (Fig. 2). Here, the Ojo Caliente Sandstone Member of the Tesuque Formation is approximately 300 m thick and disconformably to conformably overlain by the Chamita Formation (interbedded Vallito and Cejita Members). The Chamita Formation thins northward from the southern tip of Black Mesa, from 100 m to 10-30 m, beneath an unconformity at the base of Pliocene sediments.

The Tesuque and Chamita Formations on the west slope of Black Mesa differ in the following lithologic properties. The Ojo Caliente Member of the Tesuque Formation is composed of sandstone that is fine- to coarse-grained, subrounded, moderately to well sorted, and composed of quartz, minor potassium feldspar, and minor chert + volcanic lithic grains. The Ojo Caliente Sandstone is generally very pale brown, cross-stratified (with eolian

TABLE 2. Summary of $^{40}Ar/^{39}Ar$ results for Servilleta Basalts and sample of upper coarse ash

					Preferred Age						
Sample	**Unit**	**UTM coord (zone 13; NAD 27) m**	**Lab #**	**Irradation**	**min**	**analysis**	**n**	**%^{39}Ar**	**MSWD**	**K/Ca ± 2s**	**Age(Ma) ± 2s**
V-63-061103-djk	Lower of two flows located on NE part of Black Mesa	412,130 E 4,007,050 N	55545-01	NM-187J	Groundmass Concentrate	Plateau	6	79.2	1.6	0.0 ± 0.0	3.53 ± 0.25
V-31-041103-djk	5.5-6.0-thick flow on the NW part of Black Mesa (only one flow present).	412,160 E 4,008,210 N	55543-01	NM-187J	Groundmass Concentrate	N/A	N/A	31.1	N/A	0.5 ± 0.4	No age assigned
110604c-djk	Top of 18 m-thick Servilleta Basalt sequence at south tip of Black Mesa	400,970 E 3,996,100 N	55547-01	NM-187J	Groundmass Concentrate	Plateau	7	96.1	1.2	0.1 ± 0.2	3.34 ± 0.32
110604b-djk	Middle of 18 m-thick Servilleta Basalt sequence at south tip of Black Mesa	400,900 E 3,996,075 N	55544-01	NM-187J	Groundmass Concentrate	N/A	N/A	83.9	N/A	0.1 ± 0.1	No age assigned
Unit-5c-NWchili-sectdjk	Scattered, pebble-size consolidated ash and pumice in pebbly sand, 4.1-5.0 m above Chamita Fm base	396,252 E 3,994,437 N	57850	NM-217	biotite	LSH	17	N/A	2.7	4.9 ± 4.0	11.08 ± 0.44

Sample preparation and irradiation:

Neutron flux monitor Fish Canyon Tuff sanidine (FC-2). Assigned age = 28.02 Ma (Renne et al, 1998).

Instrumentation:

Analyses performed on a Mass Analyzer Products 215-50 mass spectrometer on line with automated all-metal extraction system.

Biotite and groundmass concentrates step-heated, using a Mo double-vacuum resistance furnace.

Sanidine, biotite and flux monitor fused or step-heated by a 50 watt Synrad CO2 laser.

Notes:

LSH = laser step heat (17 steps); Fm = Formation; Mbr = Member; N/A = Not applicable.

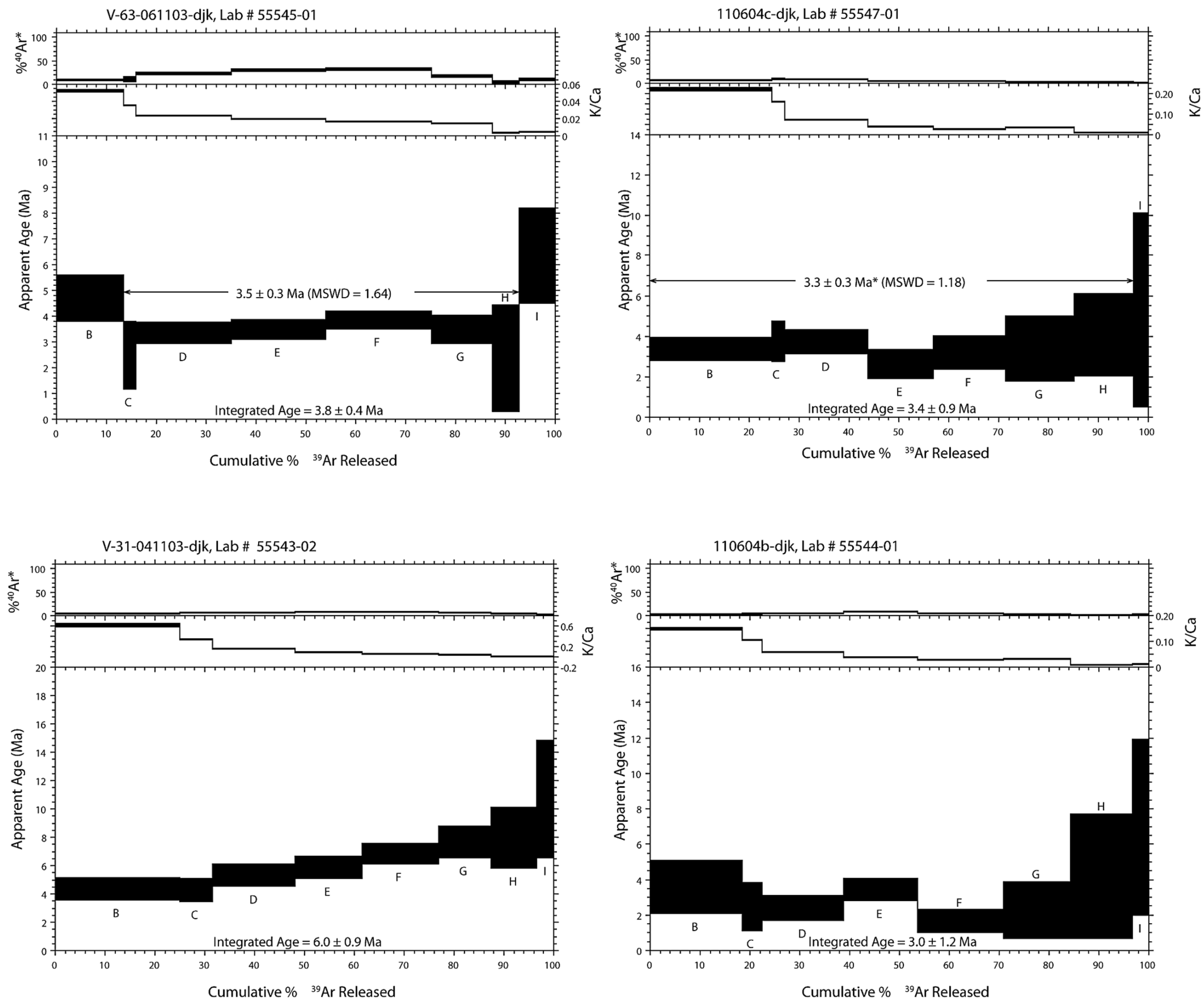

FIGURE 6. $^{40}Ar/^{39}Ar$ age spectrum plots for basalt samples on Black Mesa. The groundmass was analyzed in all four samples. See also Table 2.

foresets being thicker than 0.5 m), and contains lenticular to tabular to cigar-shaped zones of calcite cementation that locally extend across cross-bedding sets. At the mouth of the small canyon immediately south of Vallito Peak, eolian foresets are up to 8 m in thickness. The Chamita Formation is more silty than the Ojo Caliente Member of the Tesuque Formation and contains up to 30% very thin to thick, tabular beds of siltstone and claystone. This formation has sparse pebble beds whose clast assemblage consists of Paleozoic sedimentary rocks, Tertiary volcanics, and Proterozoic quartzites. The Vallito Member of the Chamita Formation has only sparse cross-stratification (<0.5 m-thick), is less cemented than the Ojo Caliente Sandstone, and contains beds that are light brown, light yellowish brown, pink, very pale brown, or light orange – generally browner than the Ojo Caliente Sandstone and becoming redder up-section. Sand in the Vallito Member is very similar to sand in the Ojo Caliente Member. A locally cross-stratified sand interval in the upper Vallito Member, at least 4 m thick and similar to the Ojo Caliente Sandstone, serves as a useful correlation unit (not depicted in Fig. 2). Interbeds of the subordinate Cejita Member are found in the Vallito Member and are lithologically similar to the Cejita Member on the Santa Clara fault hanging wall (described below). These Cejita beds become more common to the southwest.

The Vallito Member and Ojo Caliente Sandstone are illustrated in three stratigraphic sections and described further by Koning and Aby (2005) and in recent geologic mapping (Koning and Manley, 2003; Koning, 2004; Koning et al., 2005a). The West Chili stratigraphic section is located 2.5 km west of the southwestern tip of Black Mesa (Fig. 2) and includes 80 m of the upper Ojo Caliente Sandstone, Vallito Member, and Cejita Member (Fig. 8; Appendix 1). The West Chili section is capped by a basaltic lava correlated to the Lobato Basalt. This flow was dated using the $^{40}Ar/^{39}Ar$ method at 10.11 ± 0.13 Ma (Maldonado and Miggins, 2007). Located on the upper part of the west

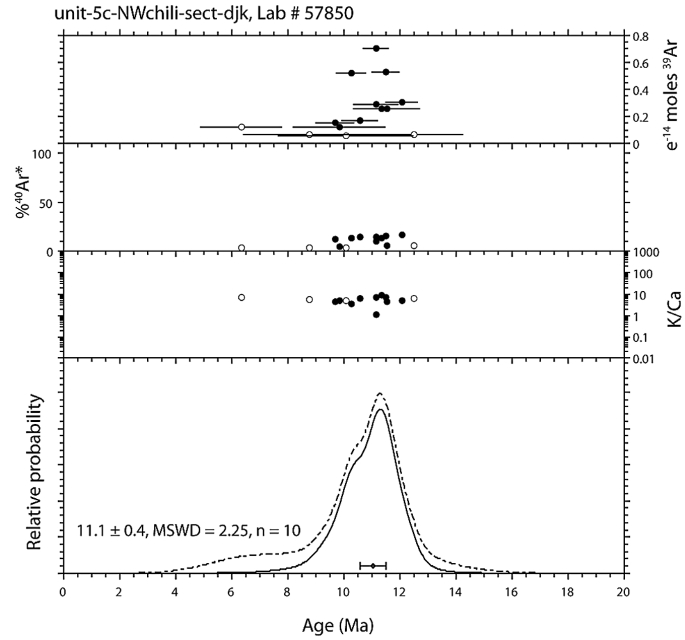

FIGURE 7. $^{40}Ar/^{39}Ar$ age probability distribution diagram for tephra sample NW-unit5c-sect-djk, collected 4-5 m above the base of the Vallito Member (Chamita Formation) at the West Chili stratigraphic section (Fig. 8). See also Table 2.

slope of Black Mesa, the Rancho de San Juan stratigraphic section encompasses 90 m of the upper Ojo Caliente Sandstone and the Vallito Member (Figs. 2 and 9; Appendix 1). The South Vallito stratigraphic section is also found on the west slope of Black Mesa, lies immediately south of the Vallito Member type section (Fig. 2), and spans 36 m across the contact between the Ojo Caliente Sandstone and Vallito Member (Fig. 10)

The basal contact of the Chamita Formation appears to be diachronous and, depending on location, varies from disconformable to apparently conformable. Unfortunately, there is no age control for both underlying and overlying strata at any single site. However, in three places there is age control for strata either below or above the contact, and based on these data it appears that the contact is diachronous. Below, we argue that the contact is 11-11.5 Ma in the south (West Chili stratigraphic section) and 9-10 Ma to the north (South Vallito stratigraphic section).

Age control for the upper Ojo Caliente Sandstone comes from two ash layers geochemically correlated to ashes dated elsewhere. A white fine ash bed was sampled in the Ojo Caliente Sandstone about 65 m below the contact (sample ML-482L-101103-djk in the Rancho de San Juan stratigraphic section; Fig. 9). Another fine white ash, mentioned in the road log of Manley and May, 1984), was sampled at the base of the west slope of Black Mesa, 8 km NNE of the first ash, and is roughly 60-70 m below the first ash. It may correlate to the 12.00 ± 0.2 Ma Cougar Point Tuff Unit V, a Trapper Creek Ash (sample ML-372a-S161003-djk in Slate et al., in review; age from Perkins et al., 1995).

The details of the electron microprobe analysis of sample ML-482L-101103-djk are summarized in Table 1 and indicate a strong correlation to the Cougar Point Tuff Unit Xl, another Trapper Creek Ash (M. Perkins, 2001, pers. communication; composition data of Perkins et al., 1995). The Cougar Point Tuff Unit X1 is 11.3 ± 0.10 Ma (Bonnichsen, 1982) and this age provides a maximum age constraint for the basal Chamita Formation contact at this location. We use sedimentation rates to obtain a more accurate age estimate of the Chamita Formation basal contact here. Given that 60-70 m of Ojo Caliente Sandstone lies between the two Trapper Creek Ashes and given the 0.7 m.y. difference in their interpreted ages, one calculates a sedimentation rate of 86-100 m/m.y. Using that sedimentation rate for Ojo Caliente Sandstone strata above the upper Trapper Creek ash at the Rancho de San Juan stratigraphic section yields an approximate age of 10.5-10.7 Ma for the basal contact of the Chamita Formation.

Age control is also available for the Vallito Member 3.6 km north of the upper Trapper Creek ash, in the vicinity of the South Vallito stratigraphic section. Here, as many as five white ash beds are mapped in the lower 90-100 m of the lower Vallito Member (Fig. 2). These fine ashes are referred to as the Vallito white ash zone (Koning et al., 2004b). A fine white ash bed at the top of the Rancho de San Juan section may correlate to the Vallito white ash zone (Fig. 11). The lowest ash bed is the thickest (up to 4.3 m) and the most laterally extensive (note that this bed is called the basal ashy stratum in Fig. 10). Individual ashes of the Vallito white ash zone are too altered for dating or chemical-based correlations. However, past workers have collected vertebrate fossils from the Vallito Member in the vicinity of Vallito Peak. These fossils include the dog *Epicyon*, the rhino *Teleoceras*, and an isolated tooth from the sloth *Pliometanastes* (Tedford and Barghoorn, 1993). The joint occurrence of *Epicyon* and *Pliometanastes* typifies fauna in the early Hemphillian North American land-mammal "age" (Tedford and Barghoorn, 1993). The sloth fossil was found in the same canyon as the South Vallito stratigraphic section, although its exact position relative to the basal Chamita contact is not known (G. Morgan, personal commun., 2011). The *rhyncotherium* specimen was collected at the base of the Vallito Member near the South Vallito stratigraphic section (Ted Galusha, unpubl. field notes).

The presence of relatively abundant white coarse ash and lapilli beds in the lower Chamita Formation on the west slope of Black Mesa, together with minor black, basaltic(?) coarse ashes, is similar to that observed in the basal Chamita Formation in the West Chili stratigraphic section and is referred to as the upper coarse ash zone in Figure 11. Thus, we are reasonably confident in correlating lower Chamita Formation strata between these two locales (Fig. 11). At the West Chili stratigraphic section, three white coarse ash beds are measured in the lower 5.6 m of the Vallito Member but are too altered for age analyses. However, a bed 6.8-7.7 m above the base of the West Chili section contains less-altered tephra dispersed in pebbly fine- to very coarse-grained sand (Fig. 8; Appendix 3). The tephra consist of very fine to fine, pebble-size fragments of consolidated white ash and pumice containing biotite and 5% unidentified mafic minerals. As described above, the biotite returned a $^{40}Ar/^{39}Ar$ age of 11.08 ± 0.44 Ma (Fig. 7). Based on this $^{40}Ar/^{39}Ar$ age and the 10.11 ± 0.13 Ma $^{40}Ar/^{39}Ar$ age of the capping Lobato Basalt at the West Chili stratigraphic section, we interpret a 10.2-11.5 Ma age range for the upper coarse ash zone and an 11.0-11.5 Ma age for the base of

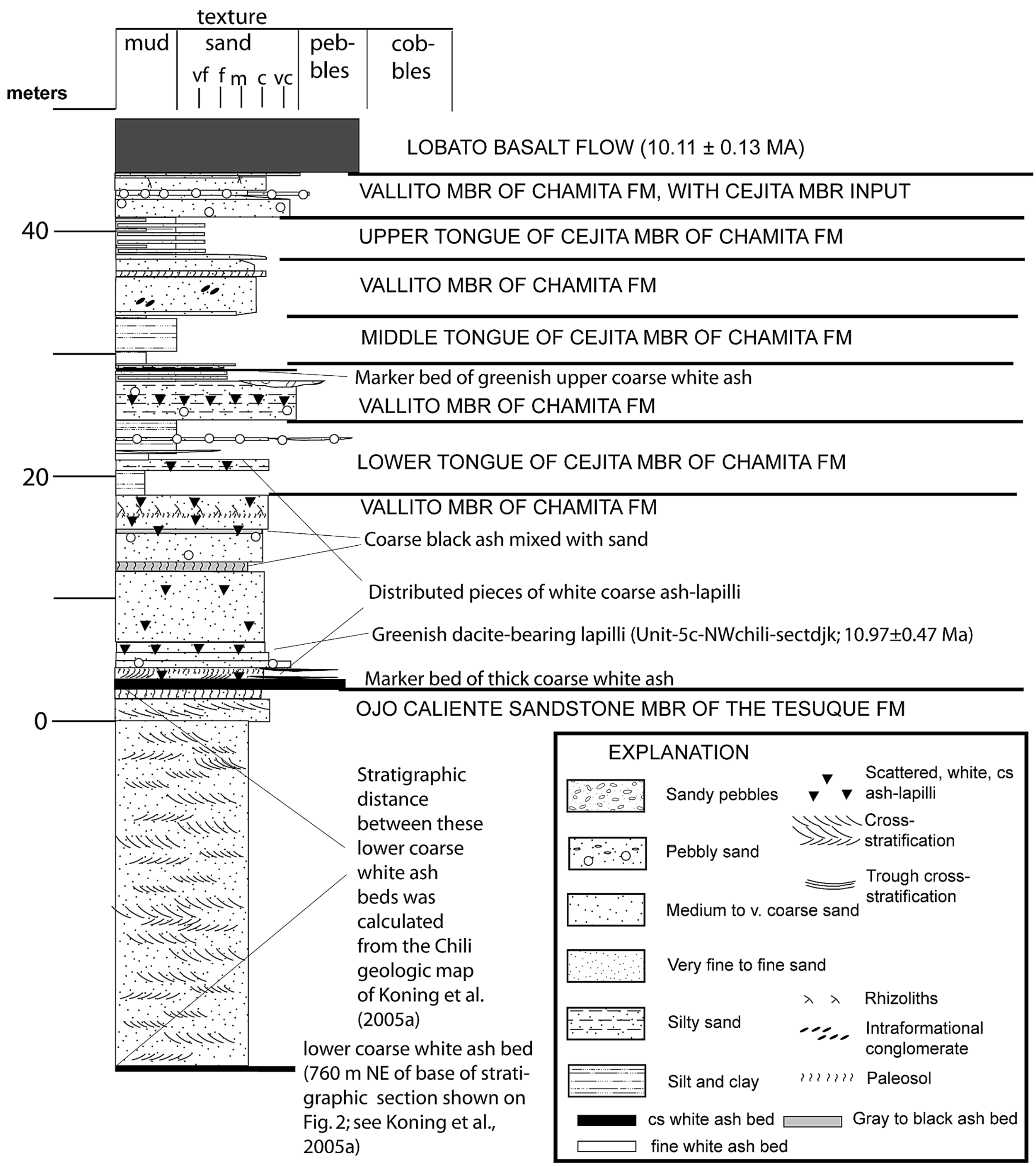

FIGURE 8. West Chili stratigraphic section. See Figure 2 and Appendix 3 for location information. Descriptive data is in Appendix 1. Lobato Basalt age is from Maldonado and Miggins (2007).

the Chamita Formation there.

The basal contact of the Chamita Formation is older to the south and disconformable there. In the West Chili stratigraphic section (Fig. 8), a weak paleosol is present at the contact that is marked by reddening and ped development. In the Rancho de San Juan stratigraphic section (Fig. 9), a paleosol is not observed

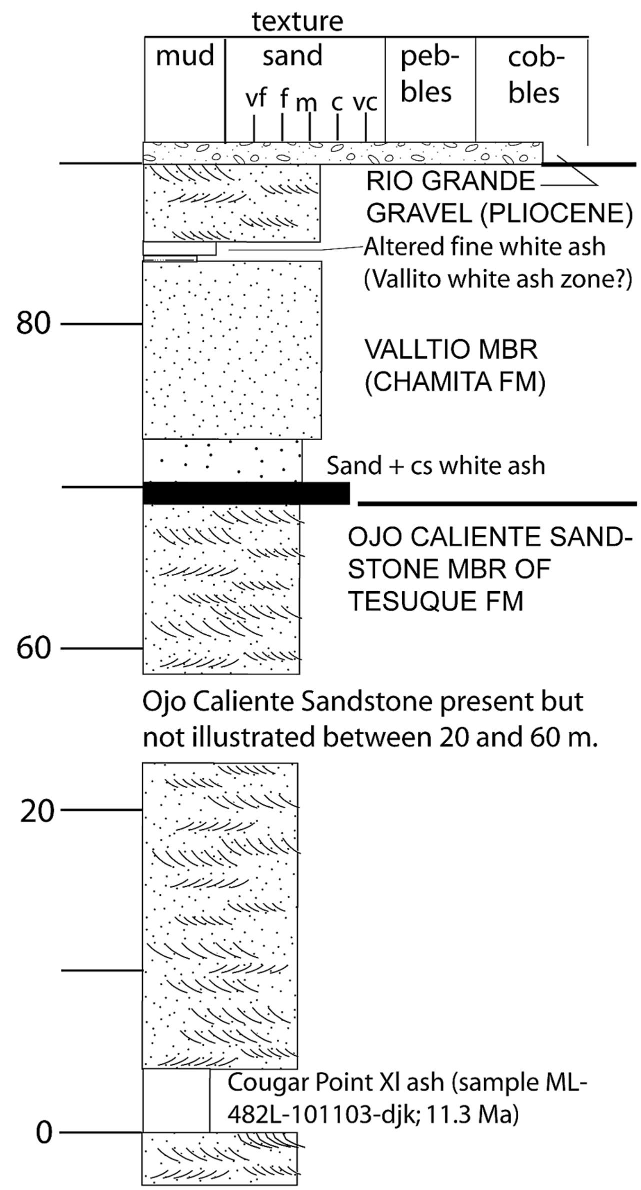

FIGURE 9. Rancho de San Juan stratigraphic section. See Fig. 2 and Appendix 1 for location information. Descriptive data is in Appendix 1. Lithologic symbols follow those in Fig. 8. Section measured using a brunton compass and eye height, so stratigraphic height errors are estimated to be ± 10%.

but the top of the Ojo Caliente Sandstone is relatively sharp and planar (Appendix 3). However, at the South Vallito section the contact appears to be gradational and conformable. Basal Vallito Member strata are approximately 11 Ma in the West Chili stratigraphic section, but fossils in the Vallito Member near the South Vallito stratigraphic section suggest an early Hemphillian (9-8 Ma) age (Tedford and Barghoorn, 1993). Although precise locations of the diagnostic *Pliometanastes* and *Epicyon* fossils are not recorded, the lower Vallito Member is the most fossiliferous so we consider it likely that the two species came from the lower Vallito Member.

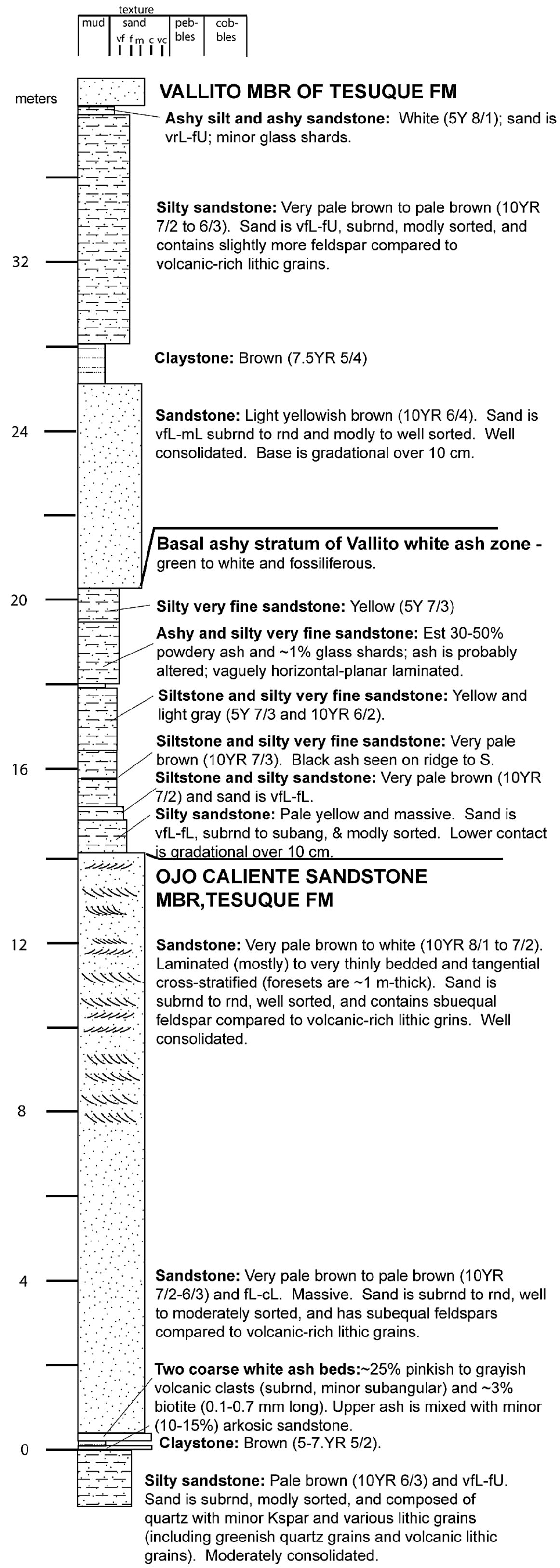

FIGURE 10. South Vallito stratigraphic section. See Fig. 2 for location. Lithologic symbols follow those in Fig. 8. Note that the Vallito Member continues above the top of the stratigraphic section. Section measured using a brunton compass and eye height, so stratigraphic height errors are estimated to be ± 10%.

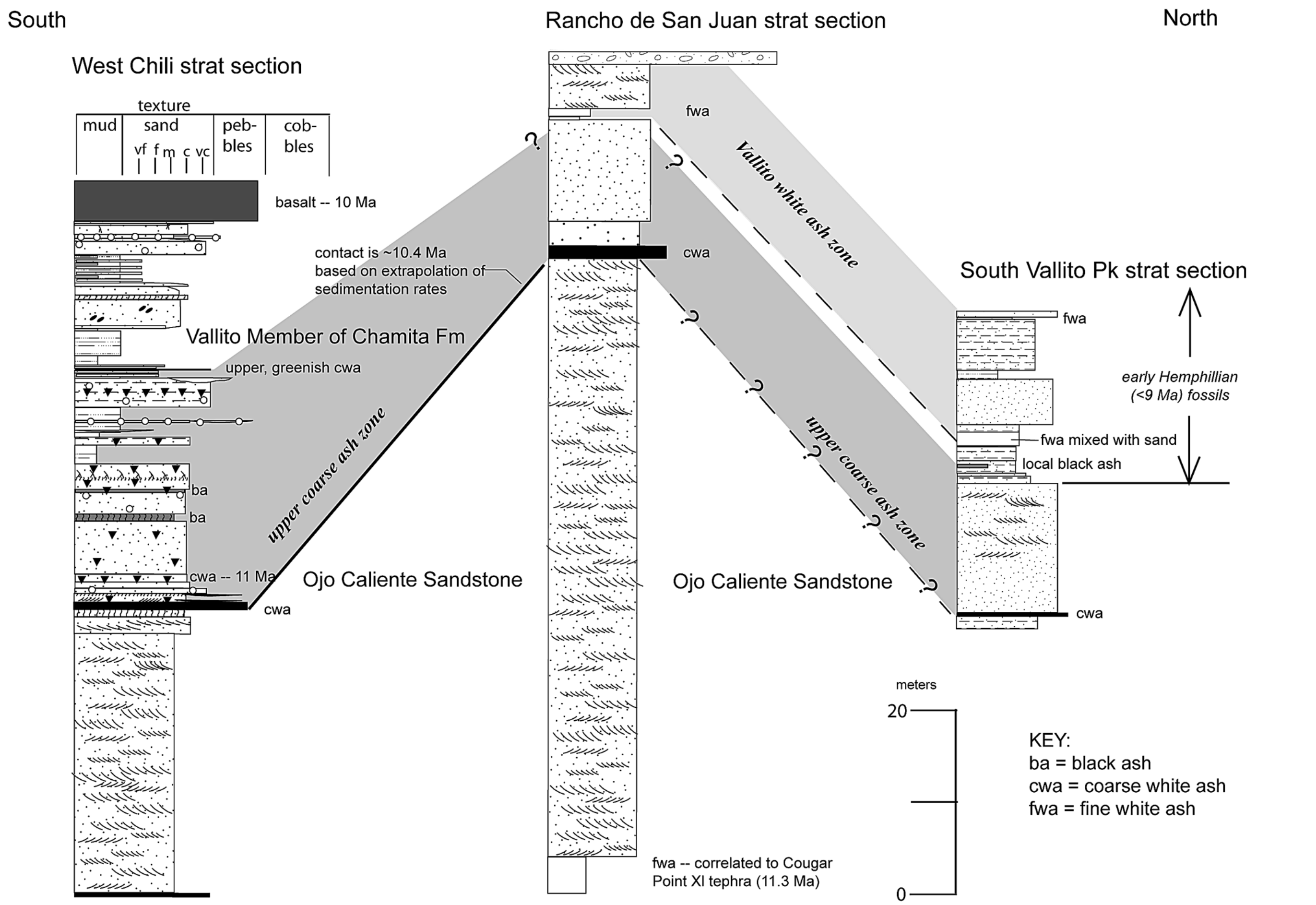

FIGURE 11. Stratigraphic correlations between the West Chili, Rancho de San Juan, and South Vallito stratigraphic sections. The Vallito and upper coarse ash zones are denoted by shading. Lithologic symbols follow those in Fig. 8.

Younger strata on hanging wall of Santa Clara fault

The Cejita and Cuarteles Members of the Chamita Formation are exposed on the hanging wall of the Santa Clara fault (Koning and Manley, 2003). As noted in the previous section, subordinate tongues of the Cejita Member strata are interbedded in the Vallito Member on the fault footwall. Based on correlation of the upper coarse ash zone, these tongues are inferred to be older than the Cejita Member exposed on the fault hanging wall (Fig. 3). Cejita and Cuarteles Member exposures on the fault hanging wall, north of the Rio Chama and west of the Rio Grande, are the type locality of the Chamita Formation (Fig. 12; Galusha and Blick, 1971; MacFadden, 1977; Koning and Aby, 2005). The Cejita Member consists of floodplain deposits of light brown, light yellowish brown, or very pale brown siltstone-claystone and fine sandstone. These fine-grained deposits are interbedded with varying proportions of coarser channel-fill deposits composed of sand and clast-supported gravel. The sand ranges in color from pale brown to very pale brown to light gray to pale yellow. The sand is fine- to very coarse-grained, subrounded to subangular, well to poorly sorted, and contains common grains of mafic, metamorphic, and Paleozoic lithic detritus (these are generally more abundant than orange-pink potassium feldspar). Gravels are clast-supported, locally imbricated, and consist of subrounded to rounded pebbles and fine cobbles. The gravel is composed of 35-60% quartzite and 15-45% green-gray Paleozoic limestone, sandstone, and siltstone (with <15% vein quartz, <10% felsic to intermediate volcanic rocks, and <15% granite). The main difference between Cejita Member and Vallito Member gravel is the paucity of volcanic clasts in the Cejita Member. The sand fraction also differs; the Cejita Member lacks chert grains and contains minor grains of Paleozoic sedimentary rocks. Paleoflow measurements from clast imbrication and channel-fill trends indicate a general southwest flow direction. It is interpreted that the Cejita Member was deposited by a river flowing southwest out of the Peñasco embayment (Manley, 1976, 1977, 1979b; Koning and Manley, 2003; Koning and Aby, 2005).

The Cuarteles Member of the Chamita Formation overlies the Cejita Member on the hanging wall of the Santa Clara fault, preserved near the core of the Chamita syncline. This member has a distinctive light brown to reddish yellow color and an arkosic composition. It consists of silty sandstone and sandy siltstone in tabular, thin to thick beds; in these beds are minor coarse- to very coarse-grained sand and locally scattered pebbles. There

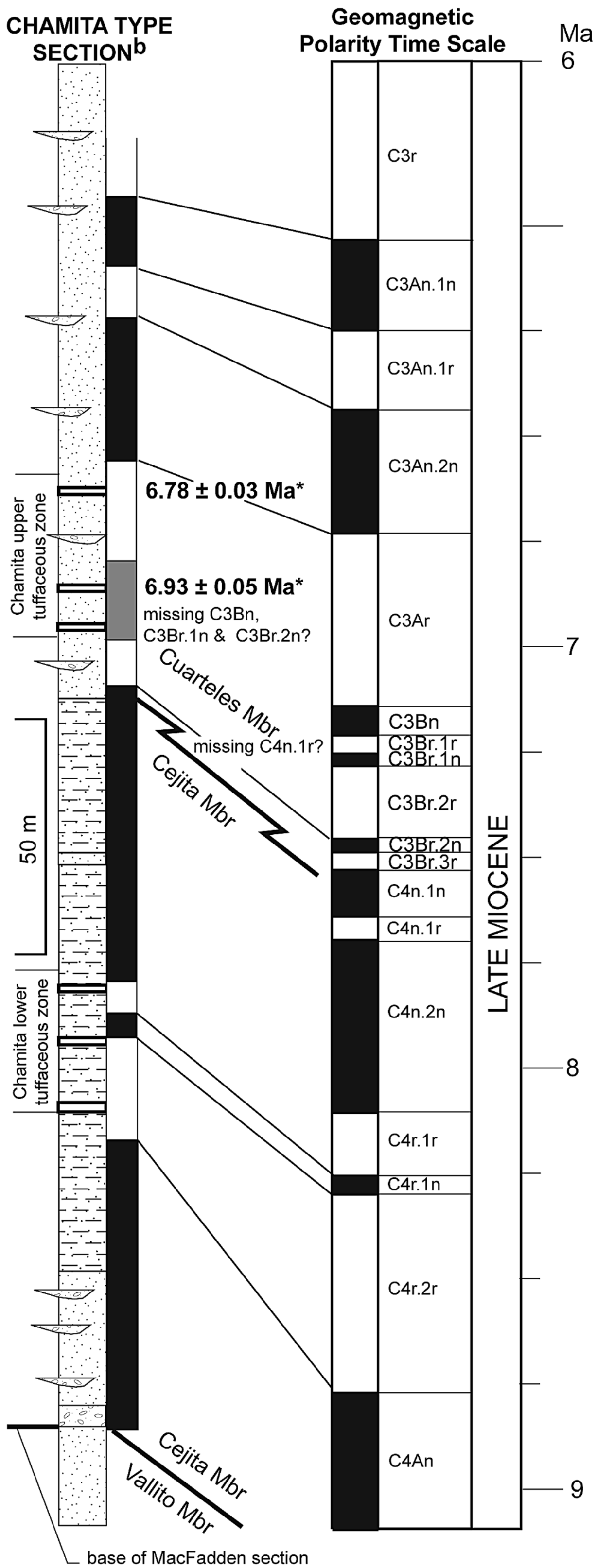

FIGURE 12. Correlation of the Chamita type section (modified from MacFadden, 1977, and McIntosh and Quade, 1995) with the geomagnetic polarity time scale of Ogg and Smith (2004). Lithologic symbols in stratigraphic sections follow those in Fig. 8, except that ashes are represented by white shading within bold rectangles. * = $^{40}Ar/^{39}Ar$ ages from McIntosh and Quade (1994).

are subordinate channel-fill complexes of pebbly sandstone and clast-supported sandy conglomerate. On the north limb of the Chamita syncline, channel-fills in the uppermost part of the Cuarteles Member are locally inset as much as 5 m into finer-grained sediment, which is much more than the ~1 m of channel scour relief typically observed in this unit. Sand is mostly very fine- to medium-grained outside of the coarser channel-fill complexes and subangular to subrounded. Gravel generally consists of subrounded to subangular pebbles, but minor cobbles are locally present. Clasts include granite with about 15-40% quartzite. Paleocurrent data indicate a west-northwest flow direction. The Cuarteles Member was deposited on a piedmont-slope in the eastern Española basin by westward-flowing streams sourced in the Sangre de Cristo Mountains (Koning and Manley, 2003; Koning and Aby, 2005).

In the badlands east of the southern tip of Black Mesa, yellowish white pumice beds are readily mappable because of their tendency to form discernable ledges. These contain coarse ash to lapilli pumice fragments that are mixed with variable amounts of detrital sand. Near the axis of the Chamita syncline is a ~40 m-thick interval where these beds are abundant and there is extensive reworking of pumiceous sand with detrital sediment (Koning and Manley, 2003). These tephra are assigned to the Chamita upper tuffaceous zone, and have been dated at 6.8-6.9 Ma using single-crystal $^{40}Ar/^{39}Ar$ methods (McIntosh and Quade, 1995). These pumice beds are mapped near the Cejita-Cuarteles Member contact on the immediate hanging wall of the Santa Clara fault, but lie higher above the contact to the east (Fig. 2). Various tephra assigned to the Chamita lower tuffaceous zone are found in the Cejita Member and are described in Koning et al. (2004a and 2005b).

Paleomagnetic and fossil studies of MacFadden (1977), revised using data and interpretations from McIntosh and Quade (1995) and a recalibrated geomagnetic polarity scale (Ogg and Smith, 2004), indicate that the Cejita Member was deposited in the Chamita type area between 9.5 and 6.8 Ma (Fig. 12). The Cuarteles Member was deposited between 7.5 and 6 Ma. Based on the relative position of the Cuarteles-Cejita contact with the Chamita upper tuffaceous zone, one can interpret relatively rapid progradation of the Cuarteles Member between 6.5 and 8.0 Ma (Figs. 2, 3, and 12).

Pliocene strata

Ancestral Rio Grande and piedmont sediment

Sediment unconformably overlying the Miocene succession and underlying the Servilleta Basalt consists of sandy gravel and sand channel-fill deposits that commonly grade upwards into silty, finer-grained sand. The gravel is clast-supported, rounded to subrounded, poorly sorted, and consists of pebbles and cobbles with local minor (5-10%) boulders. Clasts are commonly imbricated as to indicate a south to southeast paleoflow direction on western slopes of the mesa, and a southeast to southwest to west flow in gravel underlying displaced Servilleta Basalt on the east side of Black Mesa (Koning and Manley, 2003). Gravel counts at four sites (Table 3) yield: 65-86% quartzite, 0-8% reworked Miocene sandstone (only in western part of unit), 0-8% Paleozoic sandstone and siltstone, 0-1% Paleozoic limestone, 2-10% whitish to pinkish granite, 0-7% felsic to intermediate volcanic rocks, 0-7% hypabyssal porphyritic rocks, 0-1% chert, 0-1% basalt, 0-4% vein quartz, 0-8% Pilar Phyllite, and 1-2% black, mafic-rich rock and amphibolite. The amount of vein quartz and granite increases eastward (8% quartz and 14% granite in easternmost exposure). The sand is pale brown to very pale brown, very fine- to very coarse-grained, subangular to subrounded, poorly to well sorted, and arkosic to lithic-rich. Sediment is loose to weakly consolidated and weakly cemented by calcium carbonate, although locally strong cementation may be present near the base. In eastern exposures, the Pliocene sediment described above is overlain by as much as 9 m of piedmont sediment very similar to the Cuarteles Member of the Chamita Formation (Koning and Manley, 2003). This overlying sediment consists of channel-fill deposits of pebbly sand and sandy pebbles interbedded with medium to thick, tabular beds of silt and silty very fine- to very coarse-grained sand. Gravels include granite with subordinate quartzite and the sand is arkosic. Where overlain by basalt, the upper 0.1-1.5 m of the unit is commonly reddish -- probably due to chemical alteration by conduction of heat after emplacement of the overlying basalt flow. Neither an angular unconformity nor obvious (moderately to well developed) paleosol was observed at the top of the Pliocene succession, below the base of the Servilleta Basalt.

Pliocene sediment underlying the Servilleta Basalt varies in thickness, unconformably overlies Miocene sediment, and partly correlates with the Puye Formation to the south. On the west side of Black Mesa, it is 1-5 m thick and pinches out to the north. On the east side, just east of the north end of the Santa Clara fault, Pliocene sediment is 10-13 m-thick. Further south, on the hanging wall of the eastern strand of the Santa Clara fault, ancestral Rio Grande deposits and overlying piedmont deposits are 15-21 m-thick. Even on the down-thrown side of the Santa Clara fault, there is a slight (1-2°) angular unconformity between Pliocene gravels and the underlying, upper Miocene Cuarteles Member). The Pliocene sediment does not have direct age control but is inferred to be slightly older (3.8-4.5(?) Ma) than the overlying Servilleta Basalt, based on the lack of a moderately to strongly developed paleosol below the base of the basalts. The Pliocene sediment correlates, in part, with the Totavi Lentil of the Puye Formation south of the Rio Chama (Griggs, 1964; Galusha and Blick, 1971; Manley, 1979a; Waresback and Turboville, 1990).

Servilleta Basalt

The Servilleta Basalt on southern Black Mesa is a dark gray, vesicular basalt that lacks mafic phenocrysts but has abundant plagioclase laths. Vesicules are commonly in discrete zones or "pipes." A 3-8 m thick flow is exposed on the west side of the mesa. Locally this flow is overlain by another flow that is 3-6 m thick. There are generally more flows along the east side than on the west side, and the cumulative thickness on the east side is typically 10-30 m.

TABLE 3. Clast count data for Pliocene gravel near Black Mesa

Site	Location	UTM coordinates		Raw clast count data												
		Easting (m)	Northing (m)	quartzite	Santa Fe Group ss (reworked)	Paleozoic sandstone & siltstone	Paleozoic limestone	granite or gneiss	felsic to intermediate volcanic rocks	hypabyssal? porphyritic rocks	chert	basalt	vein quartz	Pilar Phyllite	mafic-rich rock, diorite, & amphibolite	other or unidentified
SCV-1312	West slope of Black Mesa	400160	3996840	65	8	7	0	8	6		1	1	3	0	1	0
SCV-2708e	East slope of Black Mesa	399398	3995245	86	0	0	0	7		1	0	0	1	1	2	1
SCV-2708m	HW of Santa Clara	399930	3994640	78	0	6	1	2	8	8	1	0	5	6	1	2*
SCV-999	HW of Santa Clara fault	401560	3994910	66	0	2	1	13	2	1	0	0	8	0		2**

Notes

* one of clasts is interpreted to be from the El Rito Formation

** one of clasts is a clear gray, cryptocrystalline silicic rock

UTM coordinates are for zone 13 and use NAD27 datum.

The age range of the Servilleta Basalt flow package on Black Mesa is interpreted to be 3.3-3.8 Ma based on three $^{40}Ar/^{39}Ar$ dates of the lower flow(s) and one $^{40}Ar/^{39}Ar$ date of the highest flow. Published $^{40}Ar/^{39}Ar$ ages from the lower flow range from 3.65 ± 0.09 Ma to 3.69 ± 0.35 Ma (Reneau and Dethier, 1996; Maldonado and Miggins, 2007). As described above, a sample of the lower flow in northern Black Mesa yielded a $^{40}Ar/^{39}Ar$ age 3.53 ± 0.25 Ma (sample V-63-061103 in Fig. 6; Table 2), consistent with results of Reneau and Dethier (1996) and Maldonado and Miggins (2007). Overlying a series of flows on the east side of the mesa are a series of eroded basalt knobs overlying ~2-3 m of gravel composed of quartzite and basalt (Fig. 2; Koning et al., 2005c). The flow capping the second knob from the south (Fig. 2) returned a $^{40}Ar/^{39}Ar$ age of 3.34 ± 0.32 Ma (sample 110604c; Fig. 6) and probably flowed in a relatively narrow channel inset into Pliocene sediment that once covered the underlying basalt flows. Except where protected by the younger basalt, this Pliocene sediment was largely removed by later erosion. There is no sign of a proximal vent facies in the basalt knobs.

DISCUSSION

Miocene-Pliocene paleogeographic evolution

During the early late Miocene, the Ojo Caliente Sandstone was being deposited in a large eolian dune field while rivers flowing from the Peñasco embayment and San Luis Basin flowed to the southwest. The southeast margin of the eolian dune field slowly retreated north-northwest between 11-11.5 Ma and 9-10 Ma (Fig. 13). To the southeast flowed the ancestral Rio Grande that deposited the Vallito Member (Fig. 13). This river mostly carried a bedload of sand reworked from the Ojo Caliente Sandstone. Even after 9 Ma, this river carried only sparse pebbles, as illustrated in

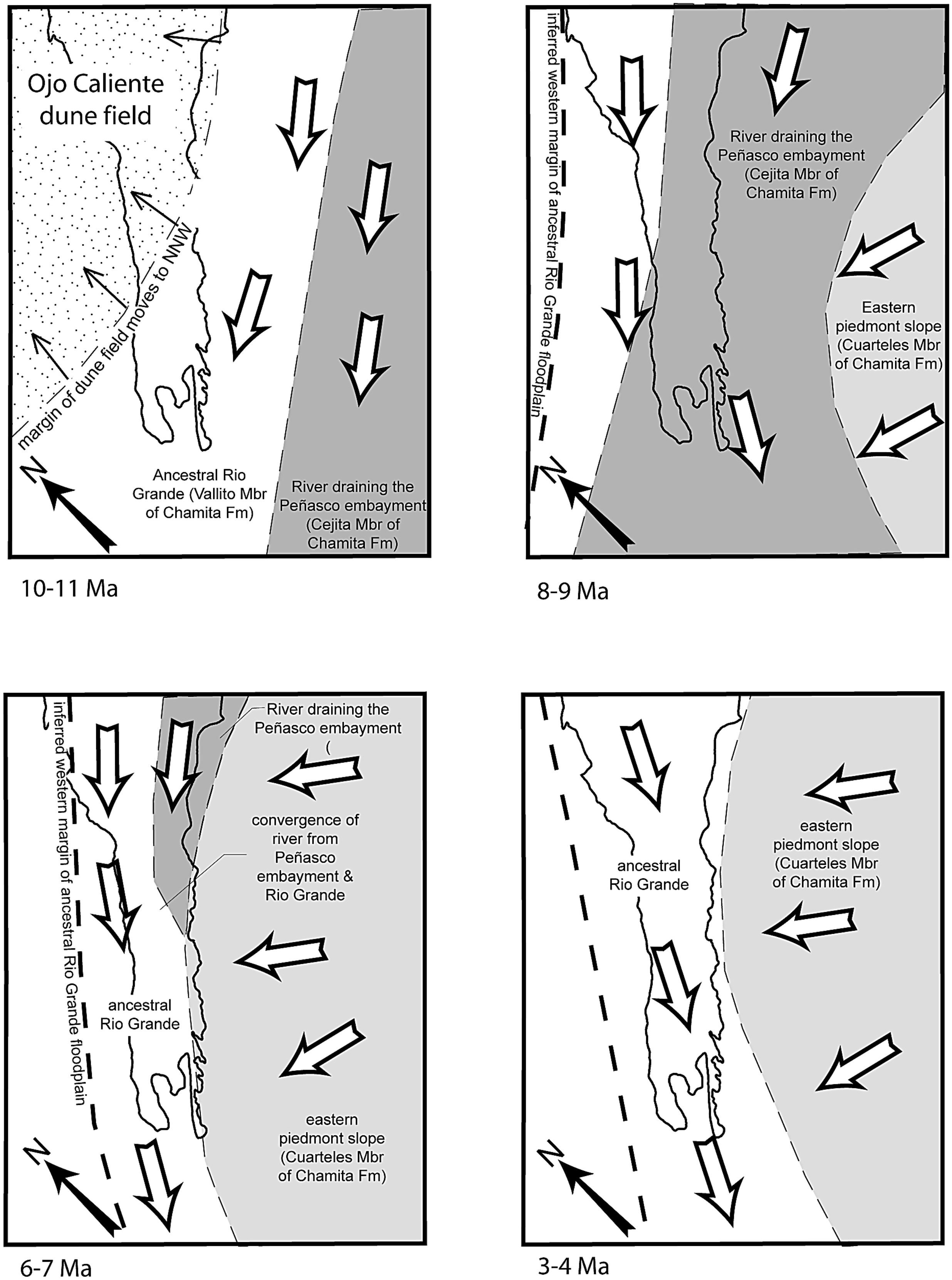

FIGURE 13. Paleogeographic map for four time periods: 10-11 Ma, 8-9 Ma, 6-7 Ma, and 3-4 Ma. Shown for reference is the boundary of the geologic map in Fig. 2 and the present-day outline of Black Mesa. Bold dashed line indicates inferred western margin of the ancestral Rio Grande; this boundary is not constrained due to late Miocene-present erosion in the Abiquiu embayment. Wide white arrows denote interpreted paleoflow of various drainage systems. Note that north is rotated 44° west of vertical.

exposures near the South Vallito stratigraphic section. To the east of the ancestral Rio Grande, a river flowed out of the Peñasco embayment that deposited the Cejita Member (Fig. 13).

Using available age control coupled with paleocurrent and map data, the lateral position of the Cejita and Cuarteles Member drainages can be tracked through time (Fig. 13). The lower to middle part of the Chamita stratotype is composed of the Cejita Member, which flanks either side of the Chamita syncline (Fig. 2). The exposed Cejita Member is 11-6.8 Ma in the study area, based on geologic mapping (Koning and Manley, 2003) and paleontologic, paleomagnetic, and radioisotopic data near the Chamita syncline (Fig. 12; MacFadden, 1977; McIntosh and Quade, 1995), as well as new radiometric age control near the West Chili stratigraphic section. During 11-7 Ma, the river depositing the Cejita Member flowed to the southwest (paleocurrent data in Koning and Manley, 2003: Koning et al., 2005a). Between 11 and 10 Ma, this river flowed onto the footwall of the Santa Clara fault as much as 3 km northwest of the Santa Clara fault (based on the presence of Cejita Member strata near the West Chili stratigraphic section (Figs. 2 and 8). The northwest margin of the river was located under southern Black Mesa, where its deposits interfinger with sandy sediment of the ancestral Rio Grande (Vallito Member). The paucity of pebble beds in the Vallito Member indicates low competency of the ancestral Rio Grande during 11-8 Ma, probably because of relatively low discharge. The southeast margin of the river associated with the Cejita Member shifted 4-5 km to the northeast shortly before, during, and after deposition of the Chamita upper tuffaceous zone (6.8-6.9 Ma). This river probably flowed under much of the current location of southern Black Mesa during 8-6 Ma (Fig. 13). Its northwest margin may have extended beyond what is now the northwestern margin of the mesa but, if so, any 6-8 Ma sediment deposited by the Cejita river was later removed by erosion on the up-thrown footwall of the Santa Clara fault.

The composition of Pliocene axial-river gravel beneath Black Mesa indicates that the river came from the north, consistent with an ancestral Rio Grande with possible input from an ancestral Rio Ojo Caliente. Gravel indicating a northerly source include Paleozoic sedimentary clasts, hypabyssal porphyritic rocks, and Pilar Phyllite. The lack of dark, intermediate volcanic clasts that typify the Rio Chama indicates that the confluence of the ancestral Rio Chama and Rio Grande was south of Black Mesa during Pliocene time.

Late Miocene-Pliocene tectonic activity

Santa Clara fault

The Santa Clara fault was active during the late Miocene and Pliocene. Koning et al. (in review) calculate throw rates between four stratigraphic markers and interpret that the period of highest throw rates after 10 Ma (70-105 m/Ma) occurred between emplacement of the Chamita lower tuffaceous zone (8.1-8.7 Ma; Fig. 12) and the Servilleta Basalt (3.3-3.8 Ma); the lowest rates (15-20 m/Ma) occurred after 640 ka. Based on the aforementioned thickness variations of Pliocene sediment across the Santa Clara fault, the hanging wall of the Santa Clara fault and possibly the Chamita syncline were actively subsiding during deposition of this sediment between 3.8 and 4.0-4.5 Ma. Preservation of younger basalt and the greater number of flows on the east side of the mesa suggests that tectonic subsidence continued during 3.3-3.8 Ma emplacement of the Servilleta Basalt.

Chamita syncline

The Chamita syncline appears to be a relatively late tectonic feature that is related to local compression in a left-step of the left-lateral Embudo fault system. On the south limb of the Chamita syncline, there is not a convincing up-section decrease in dips that would result from folding during late Miocene sedimentation (Fig. 2). However, construction of cross-sections may allow somewhat higher dips with depth (Koning et al., in review). High folding rates occurred between emplacement of the 6.8-6.9 Ma Chamita upper tuffaceous zone (Peralta Tuff) and 3.8-4.5(?) Ma Pliocene sediment under the Servilleta Basalt, based on 10-15° dip discrepancies across the angular unconformity at the base of the Pliocene sediment on the limbs of the fold (Fig. 2). A thick interval of distributed pumice near the axis of the Chamita syncline, compared to few pumice beds found on the south limb of the syncline near the Santa Clara fault, implies active down-warping of the syncline during deposition of the Chamita upper tuffaceous zone at 6.8-6.9 Ma. In contrast, the Servilleta Basalt was only deformed by 2-5° after the Servilleta Basalt was emplaced. Like the Santa Clara fault, tectonic activity of the syncline lessened after 3.3-3.8 Ma.

Regional tectonic implications

Latest Miocene-earliest Pliocene folding of the Chamita syncline and the unconformity between Pliocene and Miocene strata have regional tectonic implications. The extensive angular unconformity at the base of the Pliocene sediment, which is observed even on the immediate hanging wall of the Santa Clara fault, correlates to the unconformity at the base of the Puyé Formation to the south. This widespread unconformity indicates tectonic tilting and deformation, but relatively low sediment preservation, between 4 and 6 Ma. It is possible that epeirogenic uplift played a role in creating this unconformity. Pliocene sediments are not notably deformed, compared to underlying, tilted Miocene strata. This observation, in addition to throw rates calculated by Koning et al. (in review) for the Santa Clara fault, indicate that slip rates of the southern Embudo fault system, including deformation rates on the Chamita syncline, decreased after 4 Ma. The post 4 Ma decrease in fault slip rates, tilting, and basin subsidence was probably a rift-wide phenomena, accounting for the development of unconformities under many coarse-grained Pliocene units, including the Puyé, Ancha, Tuerto, and Ceja Formations to the south (Waresback, 1986; Waresback and Turbeville, 1990; Koning et al., 2002; Connell, 2008). The waning of tectonism along the southern Embudo fault system was probably gradual; vertical displacement rates were still sufficiently high during 3-4 Ma to cause eastward thickening of Pliocene sediment and volcanic flows. In addition to tectonic subsidence rates decreasing during the Pliocene, extensional strain narrowed (Baldridge et al., 1994; Smith, 2004; Koning et al., in review). Consequently, although the Rio Grande carried coarser-grained sediment during the Pliocene (e.g., compare the cobble-rich, Pliocene Rio Grande deposits to the sandy, gravel-poor Miocene Vallito Member), consistent with coarse Pliocene units elsewhere in the rift (Waresback and Turboville, 1990; Koning et al., 2002; Connell, 2008) and attributed to climatic variability (Zhang et al., 2001) and increased discharges, most of the sediment was carried out of the Española Basin instead of being deposited in it – creating the widespread unconformity. Preservation of thick Pliocene sediment in this part of the Española Basin was localized in the central part of the basin, in the hanging walls of the Embudo (this study) and Pajarito fault systems (Puyé Formation). Slower tectonic subsidence rates and higher-discharging rivers resulted in widespread erosion and river incision during the Pleistocene, punctuated with episodic aggradation events that produced terrace deposits along the Rio Chama and Rio Ojo Caliente. Erosion resulted in topographic inversion of Black Mesa: it occupied a low topographic position in the basin when the Servillita Basalt flowed here during 3.3-3.8 Ma, but because of Pleistocene differential erosion it now stands as a topographically high, prominent landmark.

CONCLUSIONS

Geologic mapping, tephrochronology, and $^{40}Ar/^{39}Ar$ geochronology of upper Miocene and Pliocene strata near the southern end of Black Mesa provide insight into late rift deposition and tectonism. The southeast margin of the eolian dune field associated with the Ojo Caliente Sandstone Member shifted north-northwestward between 11.0-11.5 and 9.0-10.0 Ma. To the east of the dune field, two rivers flowed southwest: the ancestral Rio Grande from the San Luis Basin and a river to the east from the Peñasco Embayment (Vallito and Cejita Members of Chamita Formation, respectively). These rivers shifted westward at the toe of a westwardly prograding piedmont-slope (Cuarteles Member of Chamita Formation) between 6 and 8 Ma. High rates of vertical displacement along the Santa Clara fault and folding of the Chamita syncline are interpreted between 7-8 and 3.3-3.8 Ma. During this time of tectonism, a hiatus in deposition occurred shortly before 4 Ma, leading to an angular unconformity between Miocene and Pliocene deposits on both the hanging wall and footwall of the Santa Clara fault. Inferred increases in discharge allowed Pliocene streams to carry coarser bedload, but preservation of sediment was largely restricted to the center of the Española Basin, including the Velarde graben. During 3.3-3.8 Ma, several Servilleta Basalt flows traveled down what was the basin floor of the Española Basin. Both the flows and underlying Pliocene sediment thicken across the Santa Clara fault, consistent with tectonic activity along this structure in the early Pliocene. After 3 Ma, tectonism along the southern Embudo fault system waned and differential erosion resulted in topographic inversion of the area covered by the Servilleta Basalt.

ACKNOWLEDGMENTS

We extend our thanks to Sean Connel, S. Judson May, and Karl Karlstrom for giving helpful reviews of earlier drafts of this manuscript. Funding for geologic mapping around Black Mesa was provided by the STATEMAP component of the National Cooperative Geologic Mapping Program.

REFERENCES

Aldrich, M.J., Jr., 1986, Tectonics of the Jemez Lineament in the Jemez Mountains and Rio Grande Rift: Journal of Geophysical Research, v. 91, no. B2, p. 1753-1762.

Aldrich, M.J., and Dethier, D.P., 1990, Stratigraphic and tectonic evolution of the northern Española Basin, Rio Grande rift, New Mexico: Geological Society of America Bulletin, v. 102, p. 1695-1705.

Bachmann, O., Schoene, B., Schnyder, C., and Spikings, R., 2010, The $^{40}Ar/^{39}Ar$ and U/Pb dating of young rhyolites in the Kos-Nisyros volcanic complex, Eastern Aegean Arc, Greece: Age discordance due to excess ^{40}Ar in biotite: Geochemistry Geophysics Geosystems, v. 11 p. 1-14

Baldridge, W.S., Ferguson, J.F., Braile, L.W., Wang, B., Eckhardt, K., Evans, D., Schultz, C., Gilpin, B., Jiracek, G., and Biehler, S., 1994, The western margin of the Rio Grande Rift in northern New Mexico: An aborted boundary?: Geological Society of America Bulletin, v. 105, p. 1538-1551.

Bonnichsen, B., 1982, The Bruneau-Jarbidge eruptive center, southwestern Idaho, *in* Bonnichsen, B., and Breckenridge, R.M., ed., Cenozoic Geology of Idaho: Idaho Bureau of Mines and Geology, Bulletin 26, p. 237-254.

Bradford, S.C., 1992, Kinematics of an accommodation zone in the Rio Grande rift; the Embudo fault zone, northern New Mexico [M.S. thesis]: Columbus, Ohio State University, 177 p.

Compton, R.R., 1985, Geology in the field: New York, John Wiley & Sons, Inc., 398 p.

Connell, S.D., 2008, Refinements to the stratigraphic nomenclature of the Santa Fe Group, northwestern Albuquerque basin, New Mexico: New Mexico Geology, v. 30, no.1, p. 14-35.

Faulds, J.E., and Varga, R.J., 1998, The role of accommodation zones and transfer zones in the regional segmentation of extended terranes, *in* Faulds, J.E., and Stewart, J.H., eds., Accommodation Zones and Transfer Zones: The Regional Segmentation of the Basin and Range province: Boulder, Colorado, Geological Society of America Special Paper 323, p. 1-45.

Ferguson, J.F., Baldridge, W.S., Braile, L.W., Biehler, S., Gilpin, B., and Jiracek, G.R., 1995, Structure of the Española Basin, Rio Grande Rift, New Mexico, from SAGE seismic and gravity data: N.M. Geological Society, 46th Field Conference Guidebook, p. 105-110.

Galusha, T., and Blick, J.C., 1971, Stratigraphy of the Santa Fe Group, New Mexico: Bulletin of the American Museum of Natural History, v. 144, 127 p.

Gonzales, M.A., 1993, Geomorphic and neotectonic analysis along a margin of the Colorado Plateau and Rio Grande rift in northern New Mexico [Ph.D. thesis]: Albuquerque, University of New Mexico, 302 p.

Griggs, R.L., 1964, Geology and groundwater resources of the Los Alamos area: U.S. Geological Survey Water-supply Paper 1753, 107 p.

Hall, M.S., 1988, Oblique slip faults in the northwestern Picuris Mountains of New Mexico; an expansion of the Embudo transform zone [M.S. thesis]: Austin, University of Texas, 69 p.

Hillman, D.M., 1986, A study of small-scale deformation features associated with the Embudo fault zone, north-central New Mexico [M.S. thesis]: Tulsa, University of Oklahoma, 83 p.

Hora, J.M., Singer, B.S., Jicha B.R., Beard B.L., Johnson C.M., de Silva, S. and Salibury, M., 2010, Volcanic biotite-sanidine $^{40}Ar/^{39}Ar$ age discordances reflect Ar partitioning and pre-eruption closure in biotite; Geology, Vol. 38, pp. 923-926.

Ingram, R.L., 1954, Terminology for the thickness of stratification and parting units in sedimentary rocks: Geological Society of America Bulletin, v. 65, p. 937-938, table 2.

Kelson, K.I., Bauer, P.W., Unruh, J.R., and Bott, J.D.J., 2004, Late Quaternary characteristics of the northern Embudo fault, Taos County, New Mexico: N.M. Geological Society, 55th Field Conference Guidebook, p. 147-157.

Koning, D.J., 2004, Geologic map of the Lyden 7.5-minute quadrangle, Rio Arriba and Santa Fe counties, New Mexico: New Mexico Bureau of Geology and Mineral Resources, Open-file Geologic Map OF-GM-83, scale 1:24,000.

Koning, D.J., Connell, S.D., Pazzaglia, F.J., and McIntosh, W.C., 2002, Redefinition of the Ancha Formation and Pliocene-Pleistocene deposition in the Santa Fe embayment, north-central New Mexico: New Mexico Geology, v. 24, no. 3, p. 75-87.

Koning, D.J., and Manley, K., 2003, revised December-2005, Geologic map of the San Juan Pueblo 7.5-minute quadrangle, Rio Arriba and Santa Fe counties, New Mexico: New Mexico Bureau of Geology and Mineral Resources, Open-file Geologic Map OF-GM-70, scale 1:24,000.

Koning, D.J., and Aby, S.B., 2005, Proposed Members of the Chamita Formation, north-central New Mexico: N.M. Geological Society, 56th Field Conference Guidebook, p. 258-278.

Koning, D.J., Ferguson, J.F., Paul, P.J., and Baldridge, W.S., 2004a, Geologic structure of the Velarde graben and southern Embudo fault system, north-central N.M.: N.M. Geological Society, 55th Field Conference Guidebook, p. 158-171.

Koning, D.J., Aby, S.B., and Dunbar, N., 2004, Middle-upper Miocene stratigraphy of the Velarde Graben, north-central New Mexico: tectonic and paleogeographic implications: N.M. Geological Society, 55th Field Conference Guidebook, p. 359-373.

Koning, D.J., Skotnicki, S., Moore, J., and Kelley, S., 2005a, Geologic map of the Chili 7.5-minute quadrangle, Rio Arriba county, New Mexico: New Mexico Bureau of Geology and Mineral Resources, Open-file Geologic Map OF-GM-81, scale 1:24,000.

Koning, Daniel J., Connell, Sean D., Morgan, Gary S., Peters, Lisa, and McIntosh, William C., 2005b, Stratigraphy and depositional trends in the Santa Fe Group near Española, north-central New Mexico: tectonic and climatic implications: N.M. Geological Society, 56th Field Conference Guidebook, p. 237-257.

Koning, D., J., Kelley, S., and Kempter, K., 2005c, Pliocene geologic features at the top of southern Black Mesa, Española basin, and a peculiar alignment of topographic knobs in the Servilleta Basalt [non-peer revived minipaper]: New Mexico Geological Society, 56th Field Conference Guidebook, p. 9-10.

Koning, D.J., Grauch, V.J.S., Connell, S.D., Ferguson, J., McIntosh, W., Slate, J.L., Wan., E., and Baldridge, W.S., *in review*, Structure and tectonic evolution of the eastern Española Basin, Rio Grande rift, north-central New Mexico, *in* Hudson, M., and Grauch, V.J.S., eds., New Perspectives on the Rio Grande rift: From Tectonics to Groundwater: Geological Society of America, Special Paper XX.

Leininger, R.L., 1982, Cenozoic evolution of the southernmost Taos Plateau, New Mexico [M.S. thesis]: Austin, University of Texas, 110 pp.

MacFadden, B.J., 1977, Magnetic polarity stratigraphy and mammalian biochronology of the Chamita Formation stratotype (Mio-Pliocene) of north-central New Mexico: American Journal of Science, v. 277, p. 769-800.

Maldonado, F., and Miggins, D.P., 2007, Geologic summary of the Abiquiu quadrangle, north-central New Mexico: N.M. Geological Society, 58th Field Conference Guidebook, p. 182-187.

Manley, K., 1976, The late Cenozoic history of the Española Basin, New Mexico [Ph.D. dissertation]: Boulder, University of Colorado, 171 p.

Manley, K., 1977, Geologic map of the Cejita Member (new name) of the Tesuque Formation, Española Basin, New Mexico: U.S. Geological Survey Miscellaneous Field Studies Map MF-877, scale 1:24000.

Manley, K., 1979a, Stratigraphy and structure of the Española Basin, *in* Riecker, R.E., ed., Rio Grande Rift: Tectonics and Magmatism: Washington, D.C., American Geophysical Union, p. 71- 86.

Manley, K., 1979b, Tertiary and Quaternary stratigraphy of the Northeast Plateau, Española Basin, New Mexico: N.M. Geological Society, 30th Field Conference Guidebook, p. 231-236.

Manley, K., and May, S.J., 1984, Third-Day road log, from Taos to Tres Piedras, Tusas, Spring Canyon, Tres Piedras, Las Tablas, Petaca, La Madera, and Ojo Caliente: New Mexico Geological Socoiety, 35th Field Conference, Rio Grande Rift – Northern New Mexico, p. 349-370.

May, J., 1980, Neogene geology of the Ojo Caliente-Rio Chama area, Española Basin, New Mexico [Ph.D. thesis]: Albuquerque, New Mexico, University of New Mexico, 204 p.

McIntosh, W.C., and Quade, J., 1995, $^{40}Ar/^{39}Ar$ geochronology of tephra layers in the Santa Fe Group, Española Basin, New Mexico: N.M. Geological Society, 46th Field Conference Guidebook, p. 279-284.

Minor, S.A., Hudson, M.R., Caine, J.S., and Thompson, R.A., *in review*, Oblique Transfer of Extensional Strain Between Basins of the Middle Rio Grande Rift, New Mexico: Fault Kinematic and Paleostress Constraints: *in* Hudson, M., and Grauch, V.J.S., eds., New Perspectives on the Rio Grande rift: From Tectonics to Groundwater: Geological Society of America, Special Paper XX.

Muehlberger, W.R., 1978, Frontal fault zone of northern Picuris Range: New Mexico Bureau of Mines and Mineral Resources, Circular 163, p. 44-45.

Muehlberger, W.R., 1979, The Embudo fault between Pilar and Arroyo Hondo, New Mexico: an active intracontinental transform fault: N.M. Geological Society, 30th Field Conference Guidebook, p. 77-82.

Munsell Color, 1994 edition, Munsell soil color charts: New Windsor, N.Y., Kollmorgen Corp., Macbeth Division.

Ogg, J.G., and Smith, A.G., 2004, The geomagnetic polarity time scale, in Gradstein, F.M., Off, J.G., and Smith, A.G., eds., A Geologic Time Scalte, Cambridge, U.K., Cambridge University Press, p. 63-86.

Perkins, M., Nash, W., Brown, F., and Fleck, R., 1995, Fallout tuffs of Trapper Creek, Idaho- A record of Miocene explosive volcanism in the Snake River Plain volcanic province: Geological Society of America Bulletin, v. 107, p. 1484-1506.

Reneau, S.L., and Dethier, D.P., 1996, Late Pleistocene landslide-dammed lakes along the Rio Grande, White Rock Canyon, New Mexico: Geological Society of America Bulletin, v. 108, p. 1492-1507.

Renne, P.R., C.C. Swisher, A.L. Deino, D.B. Karner, T.L. Owens and D.J. Depaolo, 1998, Intercalibration of standards: absolute ages and uncertainties in 40Ar/39Ar dating: Chemical Geology, v. 145, p.117-152.

Slate, J.L., Sarna-Wojcicki, A.M., Koning, D.J., Wan, E., Wahl, D.B., Connell, S.D., and Perkins, M.E., *in review*, Upper Neogene tephrochronologic correlations in the northern Rio Grande Rift, New Mexico, *in* Hudson, M., and Grauch, V.J.S., eds., New Perspectives on the Rio Grande rift: From Tectonics to Groundwater: Geological Society of America, Special Paper XX.

Smith, G.A., 2004, Middle to late Cenozoic development of the Rio Grande rift and adjacent regions in northern New Mexico, *in* Mack, G.H., and Giles, K.A., eds., The Geology of New Mexico, A Geologic History: New Mexico Geological Society, Special Publication 11, p. 331-358.

Steinpress, M.G., 1980, Neogene stratigraphy and structure of the Dixon area, Española Basin, north-central New Mexico [M.S. thesis]: University of New Mexico, Albuquerque, N.M., 127 p. plus 2 plates.

Steinpress, M.G., 1981, Neogene stratigraphy and structure of the Dixon area, Española basin, north-central New Mexico: Geological Society of America Bulletin, v. 92, p. 1023-1026.

Tedford, R.H., and Barghoorn, S.F., 1993, Neogene stratigraphy and mammalian biochronology of the Española Basin, northern New Mexico: Vertebrate paleontology in New Mexico, New Mexico Museum of Natural History and Science, Bulletin 2, p. 159-168.

Waresback, D.B., 1986, The Puyé Formation, New Mexico – analysis of a continental rift-filling volcaniclastic alluvial fan sequence [unpublished M.S. thesis]: Arlington, University of Texas, 225 p.

Waresback, D.B., and Turbeville, B.N., 1990, Evolution of a Pliocene-Pleistocene volcanogenic alluvial fan – the Puyé Formation, Jemez Mountains, New Mexico: Geological Society of America Bulletin, v. 102, p. 298-314.

Udden, J.A., 1914, The mechanical composition of clastic sediments: Bulletin of the Geological Society of America, v. 25, p. 655-744.

Wentworth, C.K., 1922, A scale of grade and class terms for clastic sediments: Journal of Geology, v. 30, p. 377-392.

Zhang, P., Molnar, P., Downs, W.R., 2001, Increased sedimentation rates and grain sizes 2–4 Myr ago due to the influence of climate change on erosion rates: Nature, v. 410, p. 891-897.

APPENDIX 1. DESCRIPTIONS OF STRATIGRAPHIC SECTIONS IN THE VICINITY OF SOUTHERN BLACK MESA, CENTRAL ESPAÑOLA BASIN.

This appendix presents descriptions of two stratigraphic sections of the upper Santa Fe Group in the central Española Basin. Colors of sediment are based on visual comparison of dry samples to the Munsell Soil Color Charts (Munsell Color, 1994). Grain sizes follow the Udden-Wentworth scale for clastic sediments (Udden, 1914; Wentworth, 1922) and are based on field estimates. Sand textures are abbreviated as in the following: very fine-lower, vfL; very fine-upper, vfU; fine-lower, fL; fine-upper, fU; medium-lower, mL; medium-upper, mU; coarse-lower, cL; coarse-upper, cU; very coarse-lower, vcL; very coarse-upper, vcU. Pebble sizes are subdivided as shown in Compton (1985). The term "clast(s)" refers to the grain size fraction greater than 2 mm in diameter. Descriptions of bedding thickness follow Ingram (1954). Each stratigraphic section was measured upsection from unit 1 using a Jacob staff and Abney level (West Chili section) or brunton compass (Rancho de San Juan section). Numerical unit designations were established up-section for measured section, but listed in descending stratigraphic order. GPS localities for sites are in UTMs (NAD 27, zone 13), errors for the sites are 4-10 m.

West Chili section. This section consists of sand with subordinate mud and pebbles of the Chamita Formation (intercalated Vallito and Hernandez Members). Section is capped by the Lobato Basalt. Measured and described on the east slope of a basalt-capped ridge 4600-4700 ft south-southwest of the capilla at the town of Chili, Chili 7.5-minute quadrangle. Measured and described by Daniel Koning on December 5, 2006 using an abney level and Jacob staff. UTM coordinates of base: 3994420 N, 0396252 E (Zone 13, NAD 27). UTM coordinates of top: 3994500 N, 0396235 E (Zone 13, NAD 27).

Unit	Description	Thickness (m) (Unit)	(Total)
	Stake D-D is labeled on a boulder with a white calcium carbonate film on its south side. This is at 19.8 m in the section. UTM coordinates of 3991333 N, 0388249 E (Zone 13, NAD 27).	19.8	
22	**Basalt flow**	3.0	47.8
	Top of section at the south tip of the basalt knob (3994500 N		
21	**Greenish phreatomagmatic deposit**	0.2	44.8
	Vallito Member of the Chamita Formation		
20	**Slightly silty sand:** vfL-vcL (mostly fU-mL), estimate 3-5% silt; pink (5-7.5YR 7/4); no internal sedimentary fabric and is probably bioturbated; sand is poorly sorted, subangular to subrounded, and composed of quartz, 15% orange-stained quartz and possible Kspar, 5-7% mafic grains, and 1-5% volcanic grains; no paleosols. Local moderate to strong calcium carbonate cementation observed near the top of the unit.	0.9	44.6
19	**Sand:** vfL-cU; reddish yellow (5-7.5YR 6/8) and internally massive; very thin bed of reddish brown (5YR 4-5/4) clay at base of unit. There are spheroidal zones in the sand (baseball to softball size) marked by 10-15% clay in the sand. This unit is disturbed and probably bioturbated; moderately consolidated.	0.3	43.7
18	**Sand:** fU-mU, very pale brown (10YR 8/2); vague, medium to thick, broadly lenticular(?) beds; sand is fU-mU, well sorted, subrounded to subangular, and composed of quartz, 12-10% orange-stained quartz and possible Kspar, 5% mafic grains, and 2-5% volcanic grains. Moderately consolidated.	1.5	43.4
	Vallito Member with Cejita Member input, Chamita Formation		
17c	**Pebbly sand:** light brown to reddish yellow (7.5YR 6/4-6); estimate 1-3% clay; pebbles consist of intermediate to felsic volcanic rocks with 30-35% Paleozoic sandstone and limestone and 10% quartz; pebbles are subrounded, moderately sorted, and up to 12 mm-long; sand is fL-vcU, poorly sorted, subrounded, and composed of quartz, minor feldspar, 4-10% volcanic grains, 5-10% mafic grains, and 1-3% Paleozoic fragments and green quartz. Weakly to moderately cemented in lower 4 cm. 20-25 cm-thick.	0.2-0.3	41.9
17b	**Sand:** fL-fU; sand continues from below and grades upward into planar-laminated to very thinly bedded silt and vfL-fL sand (beds here are commonly disturbed); 20-25 cm-thick.	0.2-0.3	41.7
17a	**Sand with 1-2% vf-f pebbles:** fU-vcU and poorly sorted; very pale brown (10YR 7/4); sand is moderately sorted, subrounded, and composed of quartz, 15% Kspar and orange-stained quartz, 3-5% volcanic grains, 5% mafic grains, and 1% green quartz or sandstone bits; gradational upper contact; 20-25 cm-thick.	0.2-0.3	41.4
	Cejita Member of the Chamita Formation		
16b	**Intercalated siltstone and very fine sandstone, with subordinate clay beds:** vfL-vfU sand; medium (mostly) to thick, tabular beds; light yellowish brown to very pale brown (10YR 6-7/4); clay is in thin to medium, tabular beds and is brown to reddish brown (5-7.5YR 5/3-4). Moderately consolidated; ~5% very thin to laminated plates of calcium carbonate.	3.2	41.2

Unit	Description	Thickness (m) (Unit)	(Total)
16a	**Freshwater limestone(?) bed overlain by a sandstone bed:** basal bed consists of 7 cm of predominately calcium carbonate; the basal bed is overlain by a 20 cm-thick, fining-upward bed of sandstone (vfL-cU, light brown to pink (7.5YR 6-7/4), planar-laminated, subangular to subrounded, and moderately sorted – lower 10 cm of this bed is weakly to moderately cemented by calcium carbonate.	0.3	38.0
	Vallito Member of the Chamita Formation		
15c	**Sandstone:** fL-cU (mostly fU-mU), fines slightly near the top of the unit; very pale brown (10YR 8/2); no sedimentary fabric (internally massive); sand is moderately sorted, subangular to subrounded, and composed of quartz, 10% orange-stained quartz and possible Kspar, 5% mafic grains, and 2-5% volcanic grains. Gradational upper contact.	1.0	37.7
15b	**Sandstone in a paleosol:** fl-cU, moderately sorted, subrounded to subangular, and approximately similar in composition to the sand in unit 5a; no sedimentary fabric. Paleosol is reddish yellow (5-7.5YR 6/6); has moderate, coarse, subangular blocky peds; peds have hard dry consistency; estimate 5-10% distributed clay (illuviated?) but no clay films, and clay content decreases downward.	0.4	36.7
15a	**Sandstone:** fU-cL; very pale brown (10YR 8/2); internally massive (no sedimentary fabric); 0.5% clay rip-ups 1-5 mm-long; sand is moderately sorted, subangular to subrounded,and composed of quartz, 12-15% orange-stained quartz and possible Kspar, 1-6% volcanic grains, and 5-8% mafic grains. Moderately consolidated. Basal part of unit consists of a 40 cm-thick channel-fill inset into unit 14 below (35 cm of scour relief); no clay rip-ups and fL-cL.	2.8	36.3
14	**Intercalated sandstone (75%) and siltstone (25%):** 9-12 cm-thick, tabular beds; silt is pink to very pale brown (7.5-10YR 7/3) and sand is pink to reddish yellow (7.5YR 7/4-6/6) and vfL-mL, well to moderately sorted, subrounded to subangular, and consists of quartz, 15% orange-stained quartz and possible Kspar, 7% mafic grains, and 3-7% volcanic grains. Well consolidated; sand may be weakly cemented.	0.4	33.5
	Cejita Member of the Chamita Formation		
13c	**Clay:** Brown (7.5YR 5/4); “gummy.”	0.2	33.1
13b	**Silt:** Very pale brown (10YR 7/4); planar-laminated and well-consolidated; local very thin beds of strong calcium carbonate cementation.	2.7	32.9
13a	**Clay:** Brown to light brown (7.5YR 5-6/3); moderately consolidated and “gummy;” local very thin beds of strong calcium carbonate cementation.	1.1	30.2
	Vallito Member of the Chamita Formation		
12	**Upper coarse white ash gradationally overlain by clayey sand**: @29.1 m: Unit is capped by a 3 cm-thick, strongly cemented, broadly lenticular bed of fL-mL, moderately sorted, subrounded to subangular sandstone of quartz, 12-15% orange-stained quartz and possible Kspar, 7-10% mafic grains, 3-5% volcanic grains, and trace to 1% green quartz grains. @28.7-29.1 m: Light brown to reddish yellow (7.5YR 6/4-6), clayey vfL-fU sand mixed with 25% cL-vcU sand-size detritus of the upper coarse white ash at the base of this unit. @28.5-28.7 m: 16 cm-thick bed of coarse white ash has 25-30% subequal biotite (altered to chlorite) compared to lithics (gray to pink but mostly gray volcanics); the biotite and lithic grains are mixed with consolidated white ash and plagioclase. Greenish white color. Gradational upper contact. Sampled this tephra at UTM coordinates of 3994475 N, 396243 E ± 7 m.	28.5	29.1
11	**Intercalated siltstone and fine sandstone:** sand is vfL-fU; pale brown to light yellowish brown (10YR 6/3-4 and 2.5Y 6/3). @27.9-28.5 m: very pale brown (10YR 7/3-4) sand similar to that in unit 10 but locally pink to reddish yellow (7.5YR 7/4-6).	0.9	28.5

Unit	Description	Thickness (m) (Unit)	(Total)
10	**Silty sand:** fL-cU sand with 1-10% vfL-vfU sand and estimated 3-5% silt; ~1% subrounded, light gray dacite very coarse sand similar to "vc"-type lithology found in the Chama-El Rito Member of Tesuque Formation; very pale brown to pink (10-7.5YR 7/3); thin to thick, broadly lenticular beds. Sand is moderately sorted, subrounded to subangular, and composed of quartz, 12-18% orange-stained quartz and possible Kspar, 5-8% mafic grains, and 3-5% volcanic grains. @27.3-27.6 m: Channel-fill of fU-vcU sand that is subrounded, moderately sorted, and composed of quartz, 8-10% orange-stained quartz and possible Kspar, 10% pink to gray, intermediate to felsic volcanic grains, and 2% green quartz grains. @26.1-26.4 m: This sand is mixed with abundant light gray to green, subrounded to subangular dacite in addition to abundant c-vc sand-size and vf- to m-pebble-size, white, biotite-bearing (~3% biotite) pumice lapilli. **This is a fluvially reworked, white, coarse white ash-lapilli bed.**	24.7	27.6
	Cejita Member of the Chamita Formation		
9f	**Siltstone:** Light brown to light yellowish brown (7.5-10YR 6/4).	1.5	24.7
9e	**Sandstone with local pebbles:** Lenticular, 20 cm-thick channel-fill of fL-mL sandstone; local very thin lenses of vf-f, subrounded pebbles and mU-vcU sand; pebbles and mU-vcU sand consist of Paleozoic sedimentary clasts (sandstone, limestone, and siltstone) together with light gray felsic-intermediate volcanic clasts; fL-mL sand is moderately sorted, subrounded, and composed of quartz, 12-15% orange-stained quartz and possible Kspar, 5% Paleozoic sedimentary grains and green quartz grains, 1-3% volcanic grains, and 5-10% mafic grains.	0.2	23.2
9d	**Silt:** Light yellowish brown (10YR 6/4); planar-lamianted to ripple-marked laminated (<1 cm-thick foresets). In lower 15 cm of this unit are very thin, lenticular beds of sandstone (well-sorted, subrounded, and composed of quartz with 10% orange-stained quartz and Kspar, 3% Paleozoic(?) green quartz grains, 2% volcanic grains, and 2% mafic grains.	1.1	23.0
9c	**Clay and mud:** Pale brown to light yellowish brown (10YR 6/3-4) to yellowish brown (10YR 5/4).	0.6	21.9
9b	**Silty sand:** vfL-cU, estimate 5% silt; pink to pinkish white (7.5YR 7/3-8/2); no internal sedimentary fabric; sand is moderately sorted, subrounded to subangular, and consists of quartz, 15-20% orange-stained quartz and possible Kspar, and 15% lithic grains (mafics, volcanics, and colored quartz (most to least)); 5% c-vc sand-size and vf-m pebble-size chunks of coarse white ash and minor gray dacite pebbles. Well to moderately consolidated.	0.9	21.3
9a	**Claystone-mudstone:** Reddish brown (5YR 5/4).	1.9	20.4
	Vallito Member of the Chamita Formation		
8	**Sand:** fL-cU; pink (7.5YR 7/4); internally massive (no sedimentary fabric); sand is moderately sorted, subrounded to subangular, and composed of quartz, 15% orange-stained quartz and possible Kspar, and 12% mafic and volcanic grains (volcanics are gray (mostly) to pink, intermediate to felsic volcanic grains with very minor black basalt(?)); estimate 5-10% vfL-vfU sand, 1-3% silt, and 1-5% vcU sand and very fine, volcanic pebbles. ~5% of sediment above the paleosol, and ~3% of sediment below the paleosol, consists of c-vc, sand-size to vf pebble-size pumice and/or consolidated white ash. Moderately consolidated and non-cemented. 16.9-17.7 m: Zone of rhizoliths; these are 2-10 mm-wide and up to 4 cm-long. @16.6-16.9 m: **paleosol:** contains 10-15% c-vc sand and vf pebble-size chinks of consolidated white ash and/or pumice; upper 10 cm is reddish brown to reddish yellow (5YR 5/4-6/6) and has strong, coarse, subangular blocky peds and has 5-10% estimated clay content; lower 20 cm is very pale brown (10YR 7/3) and has weak, very coarse, subangular blocky peds with hard dry consistence and 1-3% estimated clay;.	2.8	18.5

Unit	Description	Thickness (m) (Unit)	(Total)
7	**Sand:** fL-cL; pinkish white to very pale brown (7.5-10YR 8/2); 0.5% scattered intermediate-volcanic very fine pebbles and cU-vcU sand; no sedimentary fabric; sand is moderately sorted, subrounded to subangular, and composed of quartz, 7-10% orange-stained quartz and Kspar, 7-10% volcanic and mafic grains; moderately consolidated. @15.4-15.7 m: 8-10% fU-cU black to dark gray, basalt-andesite sand grains mixed in with the typical sand of this unit, in addition to 2-5% c-vc sand and vf pebble-size consolidated white ash-pumice grains and clasts. @ 13.5-14.0 m: Cementation similar to that in 11.1-12.0 m.	2.8	15.7
6	**Basalt-rich sand in a paleosol:** vfL-vcU (mostly fU-mU); 10-20% black to dark gray sand grains of basalt or andesite; vf-f pebbles of consolidated white ash and plagioclase with minor biotite are found within 20-40 cm from the upper contact; sand is poorly sorted, subrounded to subangular, and composed of quartz, 10-12% orange-stained quartz and possible Kspar, and 10-20% black-gray basalt-andesite grains. Sampled. @12.6-12.9 cm: reddish yellow (5YR 6/6); 1-3% clay; moderate, coarse to very coarse, subangular blocky peds; hard dry consistence; no clay films, but distributed clay within the peds may still be illuviated. Call this a Bw or Bt horizon. Photos. @12.3-12.5 cm: light brownish gray to very pale brown (10YR 6/2-7/3); coarse to very coarse, subangular blocky peds; hard dry consistence.	0.6	12.9
5d	**Sand with trace scattered pebbles:** fL-vcU (mostly mU-cL); pink (7.5YR 7/3); internally massive (no sedimentary fabric); pebbles are vf-m and similar in composition to those in the white lapilli-coarse ash beds lower in the section (i.e., gray hornblende-dacite and brown hornblende-andesite(?); sand is poorly sorted, subrounded, and consists of quartz, 7-8% orange-stained quartz and possible Kspar, and 7-8% lithic grains (volcanic with minor mafics); moderately consolidated. @11.1-12.0 m: Golf- to softball-size, calcium carbonate-indurated, sandstone balls that are commonly fused or cemented together.	4.6	12.3
5c	**Sand with scattered lapilli:** Sand is similar to unit 5a, but mixed with vf-f pebble-size chunks of consolidated white ash and plagioclase (containing 5% unidentified mafic and biotite grains) together with vf-m pebbles of dacite, including a green plagioclase-porphyritic dacite that reminds me of the lapilli clasts in one of the coarse white ash beds in the Cuarteles section; I sample the clasts; internally massive (no sedimentary fabric).	0.9	7.7
5b	**Sand:** fU-cU; very pale brown (10YR 8/2-7/3); internally massive (no sedimentary fabric); sand is similar to Ojo Caliente Sandstone (Tesuque Formation) and is poorly sorted, subrounded, and consists of quartz, 10% orange-stained quartz and Kspar, and 10% mafic grains and subordinate intermediate-felsic volcanic grains.	0.6	6.8
5a	**Sand with 0.5% pebbles:** fU-vcU; pinkish white to very pale brown (10-7.5YR 8/2); internally massive (no sedimentary fabric); pebbles are 2-10 mm in diameter and consist of light gray to pink, hornblende-dacite. Sand is poorly sorted, subrounded (mostly) to subangular, and consist of quartz, 12-15% orange-stained quartz and Kspar, and 8-10% intermediate volcanic and mafic grains with minor chert and colored quartz grains.	0.6	6.2

Unit	Description	Thickness (m) (Unit)	(Total)
4	**Slightly silty sand with ~0.5% pebbles:** vfL-vcU (mostly fU-cL), estimate 1-2% silt; pink (7.5YR 7/4); planar-laminated to rippled-marked (south-facing and up to 1 cm-thick). Pebbles are up to 1.0 cm-long and scattered in the sediment; a minor component of the pebbles consists of consolidated crystalline, coarse and fine ash; rest is dark brownish gray andesite to basalt, and lesser pink and gray, hornblende dacite like those found in the lower coarse white ash zone in the area. Sand is poorly sorted, subrounded to subangular, and composed of quartz, 15% orange-stained quartz and Kspar, and 10% lithic grains (mafics and subordinate volcanics). Moderately consolidated and non-cemented. The upper 4 cm of unit consists of reddish brown to light reddish brown (5YR 5-6/4) clayey vfL-fL sand mixed with scattered, white coarse ash-fine lapilli fragments. @4-6 cm from top of unit is a 2 cm-thick lense of **white fine lapilli-coarse white ash**; this tephra contains 5% biotite and 3% volcanic lithic grains-clasts. @6-13 cm from top of unit: **Paleoso**l: Light brown to pink (7.5YR 6-7/4); moderate, very coarse, subangular blocky peds; very hard dry consistence; no clay films. 4.6-4.7 m: thin lense of **white fine lapilli-coarse ash** (3994432 N, 396251 E, ± 6); upper 3 cm is altered to a greenish gray color; tephra consists of consolidated, fresh-looking coarse white ash and plagioclase with 3% biotite and 7% pebble-size ltihic grains; tephra is located at 95-103 cm from the top of unit.	2.1	5.6
	Lower coarse white ash zone within the Chamita Formation		
3	**White coarse ash-lapilli:** Lowermost 2 cm is strongly cemented and locally contains abundant (25-30% by volume) purple, pink, tan, and gray, vfL-c pebble-size, lithic fragments; these decrease in abundance up-section, while brown, detrital (?) clay increaseses upsection within this unit. Top is relatively planar, but base has 40 cm of wavy relief that corresponds with 40 cm of paleotopgraphic relief.	0.8	3.5
	Ojo Caliente Sandstone Member of the Tesuque Formation		>2.7
2	**Sand of a paleosol:** fL-cU (mostly mL-cL); pink (7.5YR 8/3-7/4); internally massive; sand is moderately to poorly sorted, subrounded, and composed of quartz with 12% orange-stained quartz and possible Kspar, 10-12% lithic grains (volcanics with subordinate mafics and colored quartz). Unit consists of a weak soil with weak, coarse, subangular blocky peds with no clay films; slightly hard and slight reddening.	0.9	2.7
1	**Sand:** mU-cU, very pale brown (10YR 8/2); laminated to very thin, planar to very low-angle cross-stratified beds (up to 2 cm-thick). Sand is well-moderately sorted, subrounded (mostly) to rounded, and consists of quartz, 10% orange-stained quartz and possible Kspar, 7% volcanic grains, and 8% chert and other colored quartz. Weakly consoliated and generally non-cemented (~1-3% local strong cementation).	0	1.8
	Base of section is in the uppermost Ojo Caliente Sandstone of the Tesuque Formation. UTM coordinates of: 3994420 N, 0396252 E (Zone 13, NAD 27). From here, I proceed N20°W and use 0.5° down-dip.		

Rancho de San Juan section. This section consists of sand and interbedded tephra beds of the Vallito Member of the Chamita Formation (top) and the Ojo Caliente Sandstone Member of the Tesuque Formation (bottom). Above top of section lies colluvium and then ~5 m(?) of Servilleta Basalt. Section described on the northwest slope of Black Mesa, 1 km northwest of Rancho de San Juan hotel and restaurant. Measured and described by Daniel Koning on October 11, 2003 using a brunton compass and eye height. Because of lack of precision in measurement, total thicknesses are given in two significant figures and stratigraphic height errors are estimated to be ± 10%. UTM coordinates of base: 401215 m N, 3998423 m E (Zone 13, NAD 27). UTM coordinates of top: 401360 m N, 3998300 m E (Zone 13, NAD 27).

Unit	Description	Thickness (m) (Unit)	(Total)
10	**Rio Grande gravel:** Not described in detail.	1.5	92
	Vallito Member of the Chamita Formation		
9	**Sand:** Cross-laminated and similar to sand in the Ojo Caliente Sandstone.	4.8	90
8	**Ash:** Fine white ash that is altered.	0.9	85
7	**Mudstone:** Green-gray.	0.3	84
6	**Sand:** Very pale brown (10YR 7/3-4), mL-mU sand that is massive or locally planar-horizontal bedded (very thin to laminated). No cross-stratification seen. Sand locally contains cL-vcU volcanic grains. Sand is rounded, well sorted, and composed of quartz, 10-15% feldspar, 10-15% colored quartz, volcanic, and mafic grains (most to least). Sand is weakly consolidated. Top of unit corresponds to a sharp contact that may be a disconformity.	11	84
5	**Coarse white ash mixed with sand:** Sand is similar to that of the Ojo Caliente Sandstone (see below). Beds are medium to thick and tabular. Approximate attitude: 010 1-5 SE	3	73
4	**Coarse white ash:** Ash contains consolidated white ash fragments, ~20% volcanic clasts (up to 6 mm-long), and 3% mU-vcU biotite grains. Ash is in a tabular bed.	1.3	70
	Ojo Caliente Sandstone Member of the Tesuque Formation		
3	**Sand:** Very pale brown, fL-mL sand that is cross-laminated; minor very thin cross-beds. Foresets are 5-6 m in height and dip 105-110 degrees (ESE). Sand is moderately consolidated, with 3% locally strongly cemented bodies 2-6 m-thick. Top of unit corresponds to a very sharp, planar contact that is likely a disconformity.	65	69
2	**Ash:** White (N8/), silty-textured, and containing abundant glass shards. The ash is horizontal-planar laminated and contains 0-1% biotite (0.1-0.4 mm long). **Sample ML-482L-101103-djk collected 2 m above base of ash.**	4.0	4.0
1	**Sand:** Very pale brown (10YR 7/2), fU-mU (mostly mL) sand that is cross-laminated. Sand is subrounded to rounded, well-sorted, and composed of quartz, 15-20% feldspar, and 12-15% mafics, colored quartz, and lesser volcanic grains.	-3	